# Self-Assembling Capsules

M. Morgan Conn[†] and Julius Rebek, Jr.*[,‡]

*Department of Chemistry, Amherst College, Amherst, Massachusetts 01002-5000, and Skaggs Institute for Chemical Biology and the Department of Chemistry, Scripps Research Institute, 10550 North Torrey Pines Rd., La Jolla, California 92037*

*Received November 14, 1996 (Revised Manuscript Received April 1, 1997)*

## Contents



## I. Introduction

Supramolecular chemistry is a branch of chemistry concerned with the coalescence of molecules into noncovalent arrays. In other words, molecular recognition. Molecular recognition relies upon the complementarity of size, shape, and chemical functionalities. It explores and exploits intermolecular forces, the weak attractions that act over short distances between molecules. These forces—hydrogen bonds, aromatic $\pi$-stacking, and polar and van der Waal's interactions—are the ones that bring molecules together into complexes. Such complexes are temporarily and weakly bound groups of two or more molecules. Molecular recognition is then intimately involved in two separate processes: the binding of one molecule by another and the assembly of multiple molecules into supramolecular structures. There have been many creative contributions to the field of supramolecular chemistry in the construction of receptors, transport agents, enzyme models, and extended arrays. A several-volume series covering supramolecular chemistry far more comprehensively than is possible here has recently been published.[1]

We can define self-assembling capsules as receptors with enclosed cavities that are formed by the reversible noncovalent interaction of two or more, not necessarily identical, subunits. The aggregate so formed should have a well-defined structure in solution and be capable of binding behavior that none of its individual components display alone. This definition naturally places an emphasis on three-dimensional assemblies. It specifically excludes indefinite arrays and aggregates that are not designed to act as receptors such as micelles, liquid crystals, monolayers, metal−ligand structures, and assemblies that exist only in the solid state. As such, self-assembling capsules represent a subset of self-assembling systems. For a more general overview of self-assembly, the reader is directed to some excellent recent reviews on the subject.[2,3]

## II. Hydrogen-Bonded Systems

Hydrogen bonding is the favorite intermolecular force in self-assembling systems by virtue of its directionality, specificity, and biological relevance.[4] We can think of a viroid capsule as the ultimate self-assembling receptor—nucleic acids and sometimes proteins packaged up in a robust, precise geometric assembly of multiple protein subunits. It is our desire to understand and repeat this achievement that drives much of these studies.

Two-dimensional hydrogen-bonded arrays are enormously popular in supramolecular chemistry.[5−7] For the most part, these systems use rigid, flat, heterocyclic compounds. For example, a two-dimensional system of three molecules illustrates some of the features of self-complementarity involved in assembly. The structure designed and synthesized by Zimmerman (Figure 1) presents a pattern of hydrogen-bond donors and acceptors on one edge that is complementary to the pattern on the other functioning edge.[8] Accordingly, assembly at one level can be predicted. The spatial orientation of the atoms capable of hydrogen bonding at both edges of the molecule is fixed at almost exactly 120° by the rigidity of the aromatic centerpiece of the structure. The information for the assembly is written into the hydrogen-bond patterns of the edges and their angular orientations with respect to each other. In solution a trimer is formed, and the assembly process takes place in the self-correcting (cooperative) manner expected. Our concern, then, is how the information for *three*-dimensional assembly is structurally encoded so that discrete aggregates are formed at the expense of extended arrays.

[†] Amherst College.
[‡] Scripps Research Institute.

S0009-2665(96)00380-9 CCC: $28.00 

M. Morgan Conn was born in New York State in 1968. In 1971, his family returned to Canada and he grew up in both Vancouver and southern Ontario. He attended Trinity College at the University of Toronto and received his B.Sc. degree in 1989. After joining the research group of Julius Rebek at the Massachusetts Institute of Technology in that year, he received the Ph.D. in 1994 for studies on the molecular recognition of adenosine derivatives. He was a Miller Research Fellow in the laboratory of Peter G. Schultz at the University of California, Berkeley (1994–1996) where he used *in vitro* selection to isolate new catalytic RNA sequences. In the summer of 1996, he joined the Chemistry Department at Amherst College, a primarily undergraduate liberal arts college. The students in his research group are using combinatorial and traditional organic synthesis to study molecular recognition in biological systems.

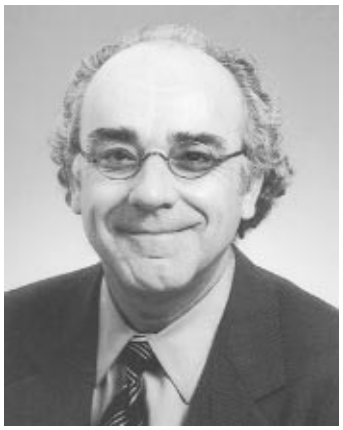

Julius Rebek, Jr. was born in Hungary in 1944 and lived in Austria from 1945 to 1949. He and his family then settled in the United States in Kansas. He received his undergraduate education at the University of Kansas in 1966, and obtained the Ph.D. degree from the Massachusetts Institute of Technology (1970) for studies in peptide chemistry with Professor D. S. Kemp. As an Assistant Professor at the University of California at Los Angeles (1970–1976) he developed the "three-phase test" for reactive intermediates. In 1976, he moved to the University of Pittsburgh where he rose to the rank of Professor of Chemistry and Chairman of the organic division. In 1989 he returned to the Massachusetts Institute of Technology, where he was the Camille Dreyfus Professor of Chemistry. In July of 1996, he moved his research group to The Scripps Research Institute to become the Director of The Skaggs Institute for Chemical Biology, where he continues to work in combinatorial chemistry and self-assembling systems.

## A. Restrained Aggregates

One productive strategy in the construction of self-assembling receptors has been the truncation of infinitely associating aggregates. Although none have been used as receptors, these systems are included because of the lessons they have taught on reducing infinite arrays to discrete, predictable assemblies. These considerations are important in the design of new and more complex receptors.

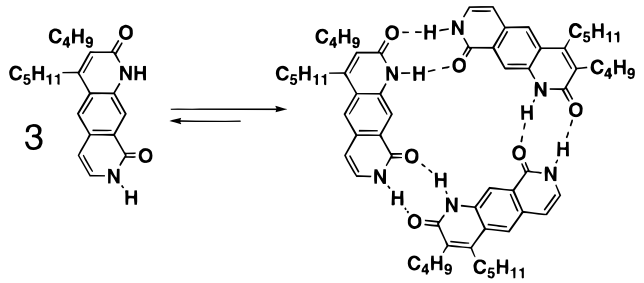

**Figure 1.** A two-dimensional assembly based upon self-complementary hydrogen bonding.

### *1. Self-Assembling Dendrimers*

Zimmerman has recently reported a three-dimensional self-assembling system where self-assembly is controlled by dendrimer substituents.[9] As shown in Figure 2, tetraacid **1** can potentially form both cyclic and linear aggregates. On the basis of the concentration dependence of size exclusion chromatography

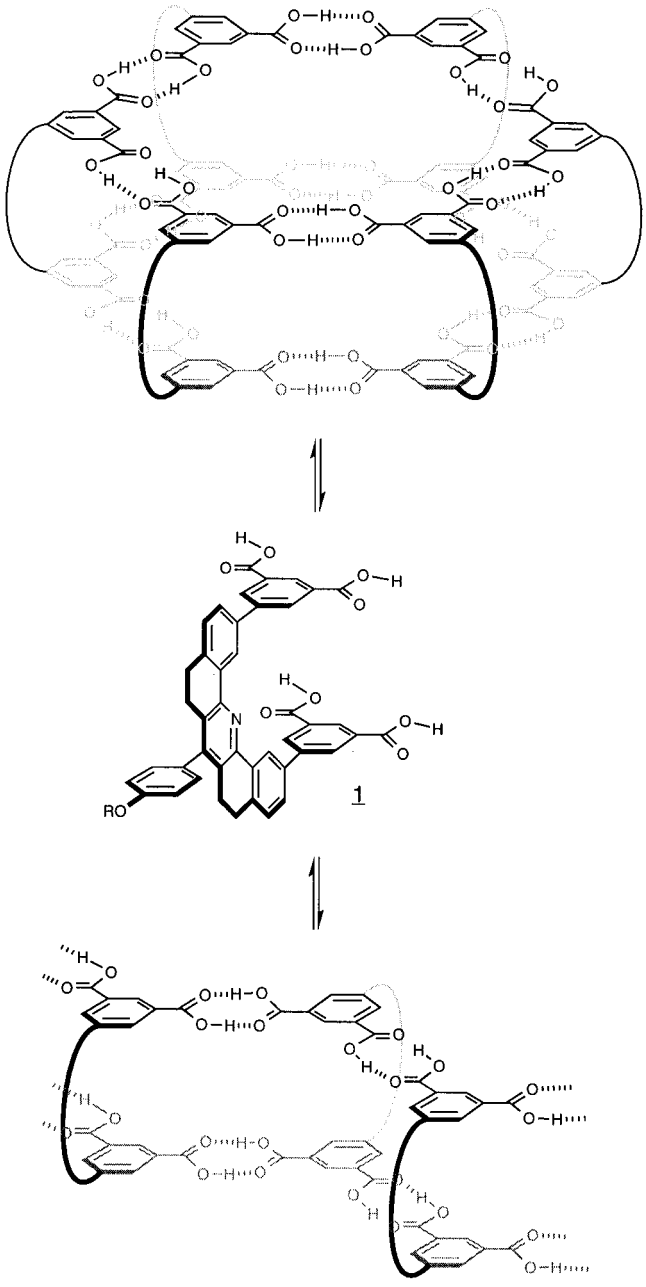

**Figure 2.** Cyclic hexamerization vs linear aggregation is controlled by the substituent (R) on diacid **1**.

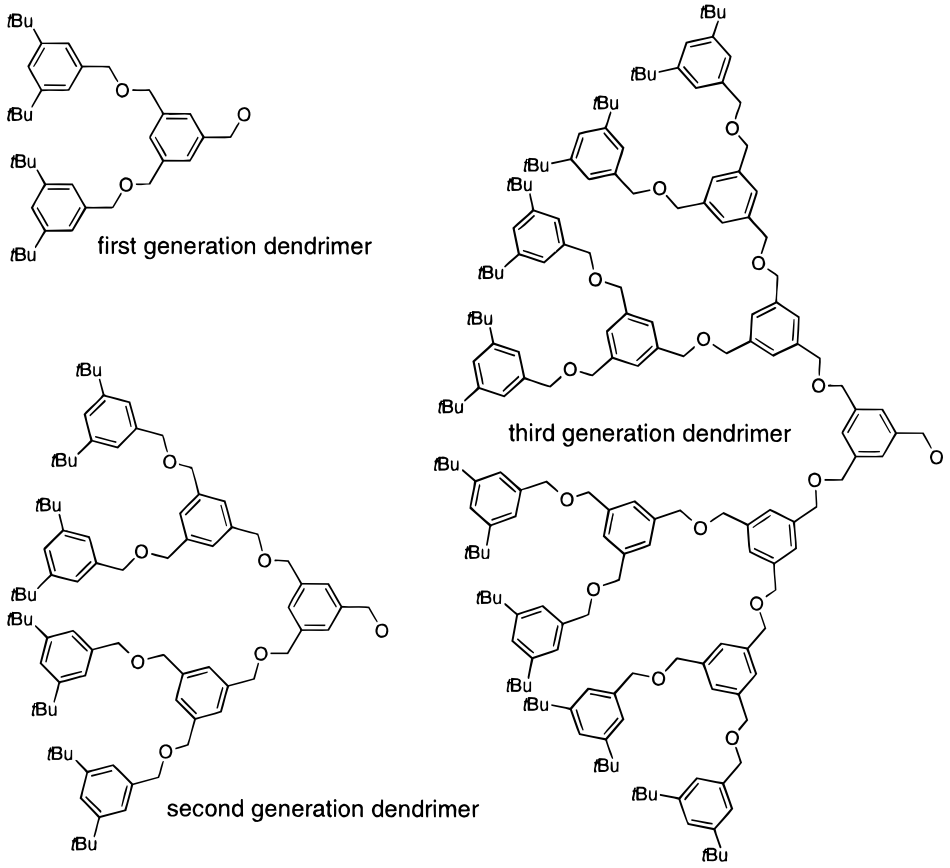


**Figure 3.** The size of the dendrimer substituent grows exponentially with each generation.

(SEC) in dichloromethane, Zimmerman and co-workers concluded that the bulk of the pendant dendrimer determines the extent to which the complicating linear aggregate is present. Size does matter, as the larger substituents (second to fourth generation dendrimers, Figure 3) clash in the linear aggregate, but not in the hexamer.

The association of these species is dependent on hydrogen bonding and, therefore, is only observed in nonpolar solvents: more competitive tetrahydrofuran precludes any self-assembly. However, it has previously been shown that clefts such as **1** are capable of binding aromatic molecules by intercalation[10] so it may be possible to exploit its hydrophobicity to drive assembly. That is, in aqueous solution, a large aromatic guest may induce the formation of the complex between itself and the hexameric aggregate. Given the recent interest in dendrimers,[11,12] the confluence of self-assembly and dendrimer fields has an exciting potential for the construction of materials with new and interesting properties.

### *2. Peptide-Based Systems*

The peptide nanotubes of Ghadiri and co-workers[13] generate three dimensionality by virtue of orthogonal hydrogen bonding. The hydrogen bonds driving the formation of the assembly are perpendicular to the plane of the individual molecule, as in a $\beta$-sheet. The amino acid side chains in naturally occurring peptide $\beta$-sheets align with their partners on other strands and alternate position between the top and bottom of the $\beta$-sheet. By incorporating alternating D- and L-amino acids in a cyclic peptide, a tube can be constructed by sheet formation, where all the amino acid side chains lie on the outer surface of the tube (Figure 4). Tube formation is driven by hydrogen-

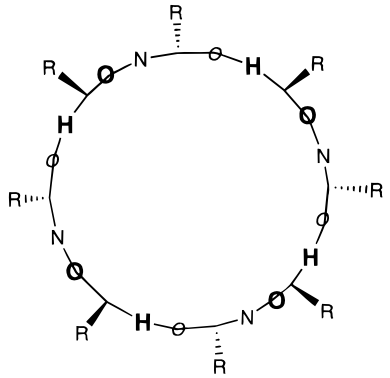

**Figure 4.** Top view of an alternating D,L-cyclic octapeptide. The macrocycle is in the plane of the page; atoms shown in bold come up out of the plane; atoms shown in italics are below the plane of the page.

bonding in nonpolar environments. Indeed, these tubes have been shown to form in phospholipid bilayers and act as channels for both ion and glucose transport.[14,15] These assemblies bear a passing resemblance to the $\beta$-helices recently observed in protein structures.[16,17]

Appropriate methylation of every other amide nitrogen controls the aggregation of these potentially infinite arrays of cyclic peptides, reducing it to a dimeric assembly (Figure 5). This clever modification made possible the detailed study of thermodynamic and structural properties of the association process.[18] As expected for an assembly driven by hydrogen bonding, the association constants are solvent dependent ($K_d$ = 71 $\mu$M in $CCl_4$ and 794 $\mu$M in $CDCl_3$) as determined by $^1$H NMR titration. The thermodynamic parameters in chloroform reflect the favorable enthalpy ($\Delta H_{298} = -11.0$ kcal/mol) of hydrogen bond-

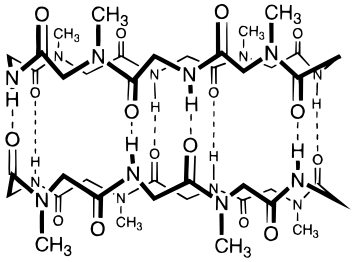

**Figure 5.** A schematic of the dimerization of two alternating D,L-cyclic octapeptides. Side chains have been removed for clarity.

ing and the unfavorable entropy ($\Delta S_{298} = -23.7$ cal/K·mol) of bringing two flexible molecules together. (Because each cyclic peptide contains four secondary amides, there are a number of slowly interconverting conformational isomers, which were observed by $^1$H NMR.) Furthermore, the results of X-ray analysis of single crystals grown from water-saturated dichloromethane confirmed all the earlier deductions. The cyclic peptides assemble by means of eight hydrogen bonds into an antiparallel oriented cylindrical dimer where the amide bonds are perpendicular to the plane of the ring. The observed intersubunit N−O distance is 2.90 Å, which correlates extremely well with the values calculated from FT-IR N−H stretching measurements. The cylinder has an internal diameter of 7.5 Å$^3$ and is filled with a number of disordered water molecules, which is indicative of the hydrophilicity of the nanotube interior. Ghadiri and co-workers suggested that the lack of specific water-binding sites may serve as a rationale for the transport efficiency of these peptide nanotubes.

This bimolecular aggregate has been used as a model to measure the relative stability of parallel and antiparallel $\beta$-sheets.[19] Cyclic peptide c[$^{Me}$aF$^{Me}$aF$^{Me}$aF$^{Me}$aF] and its enantiomer c[$^{Me}$Af$^{Me}$Af$^{Me}$Af$^{Me}$Af] each self-associate to form an antiparallel $\beta$-sheet dimer, where A is alanine, F is phenylalanine, uppercase indicates natural (L) stereochemistry and lowercase indicates unnatural (D) stereochemistry. The free energy of this association ($\Delta G_{293}$) is −4.56 kcal/mol as determined by $^1$H NMR titration in $CDCl_3$. When the two enantiomers were mixed, they also formed a mixed parallel $\beta$-sheet dimer (Figure 6). This new (diastereomeric) species appeared as an extra set of resonances in the $^1$H NMR spectrum in $CDCl_3$ and its stability ($\Delta G_{293} = -3.76$ kcal/mol) was determined by comparative integration. From this observation, Ghadiri and co-workers concluded that the antiparallel $\beta$-sheet arrangement is more favorable by some 0.8 kcal/mol by virtue of the hydrogen-bonding pattern alone. As a control for this argument, a third cyclic peptide, c[$^{Me}$aL$^{Me}$aF$^{Me}$aL$^{Me}$aF], was constructed and determined to exist as an equimolar mixture of two diastereomeric forms in $CDCl_3$, demonstrating that, in nonpolar solvents, side-chain interactions are not relevant to this difference.

The partially methylated cyclic peptides were also used to form a covalent assembly, where the self-assembly process controls the product formation.[20] When two of the phenylalanine residues of the above cyclic peptide were replaced with L-homoallylglycine (Hag), the resulting $\beta$-sheet dimer could be captured as a covalently linked macrotricyclic structure (Figure 7). Two linkages were formed in a stepwise

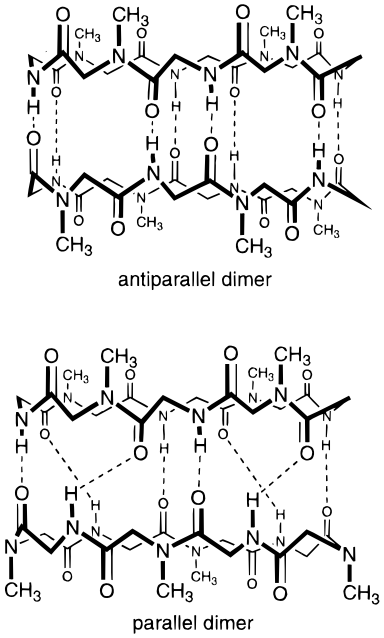


**Figure 6.** Antiparallel dimerization of c[$^{Me}$aF$^{Me}$aF$^{Me}$aF$^{Me}$aF] or c[$^{Me}$Af$^{Me}$Af$^{Me}$Af$^{Me}$Af] and the parallel dimer formed from an equimolar mixture of the two enantiomers. Side chains have been omitted for clarity.

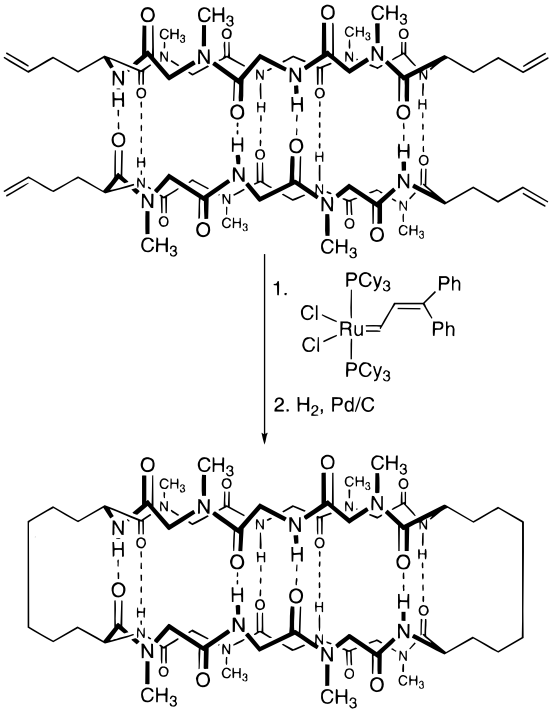


**Figure 7.** Formation of a covalently linked peptide tube by olefin metathesis.

fashion by olefin metathesis and then reduced to provide a single diastereomer of a tricyclic, intramolecularly hydrogen-bonded peptide. Spectroscopic examination (NMR, IR) of the resulting product confirmed the symmetry of the resulting complex and the regularity of the hydrogen-bonding pattern. No product was observed when the reaction was performed in more polar solvents which disrupt the hydrogen-bonded aggregate. This can be thought of as another example of the template effect,[21,22] where structure-specific molecular recognition allows formation of the desired product and prevents the formation of side products.

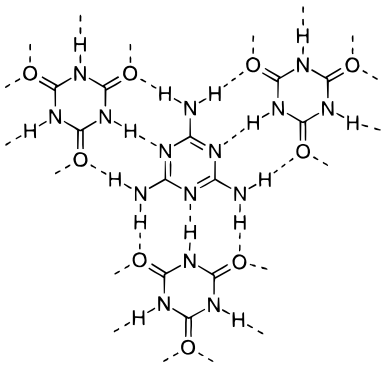

**Figure 8.** The infinite melamine−cyanuric acid hydrogen-bonded lattice.

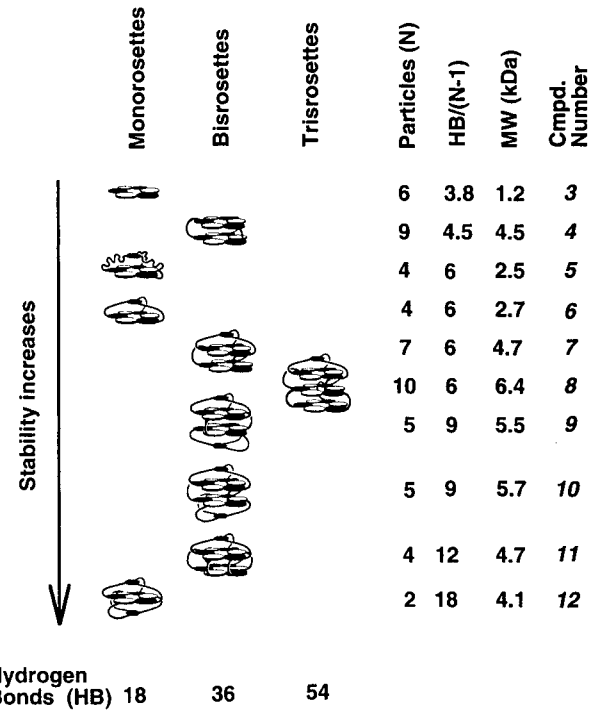


**Figure 9.** A hierarchy of restrained rosette structures. (Reprinted with permission from ref 24. Copyright American Chemical Society.)

### 3. Melamine–Cyanuric Acid Systems

The hydrogen-bonding network that forms between melamine and cyanuric acid is capable of forming infinite sheets in the solid state (Figure 8).[23] This motif has been studied extensively by the group of Whitesides.[7] Appropriate substitution of the constituents can be used to restrain the infinite lattice and produce linear or "crinkled" tapes in the solid state. Furthermore, the principles of preorganization and peripheral crowding, as reviewed by Whitesides,[24] were used to disfavor infinite aggregates and direct assembly into structurally defined (melamine)$_3$·(cyanuric acid)$_3$ aggregates, termed rosettes, in chloroform solution. Monorosettes,[25−28] bis-stacked rosettes,[29−32] and tris-stacked rosettes[33] have been assembled (Figure 9) and characterized by $^1$H or $^{13}$C NMR, vapor pressure osmometry and gel permeation chromatography.

The stability of these assemblies is a fine balance between enthalpically favorable hydrogen bonding and entropically disfavored aggregation (related to the number of particles, N, involved). Whitesides and co-workers found that the stability of their rosette

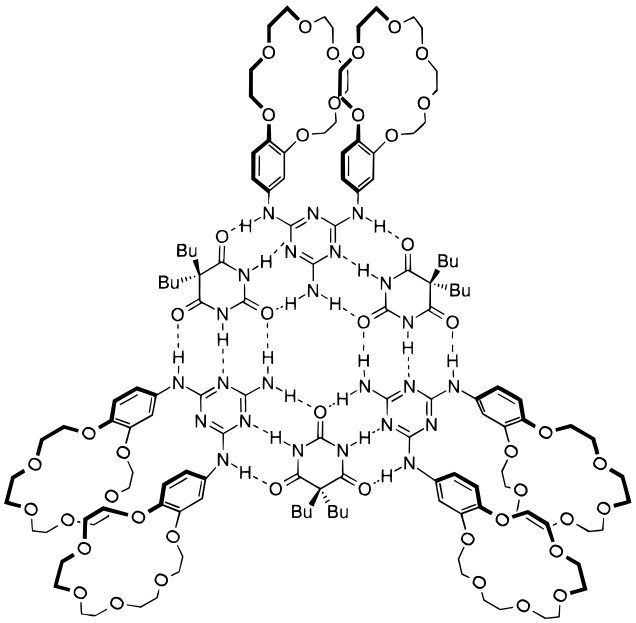

**Figure 10.** Cation-labeling of melamine−barbiturate rosettes by crown ether complexation.

structures roughly correlates with the ratio HB/($N$ − 1), where HB is the number of hydrogen bonds formed in the aggregate.[24] They have extended this observation in the development of expressions that predict the relative stability of assemblies.[34] These studies have provided a number of insights into the strategies for designing molecular assemblies; however, the structures they have examined were not designed to act as receptors.

In a related study, Lehn and co-workers were able to use electrospray mass spectrometry, a mild technique which uses no external ionization and can detect noncovalent complexes, to characterize (melamine)$_3$·(barbiturate)$_3$ rosettes by appending crown ethers from the melamine subunits (Figure 10).[35] Rosettes so functionalized can complex alkali metal cations, potassium in particular, and are detectable by ES-MS. This method, so-called ion-labeled electrospray mass spectrometry (IL-ESMS) has the potential to detect large molecular aggregates, although it is unclear how much structural or thermodynamic information it can provide. Recently, Whitesides and co-workers have also used this technique to observe their aggregates in nonpolar organic solution.[36] By using $Ph_4P^+Cl^-$ as a charge carrier, the requirement for synthetic modification was avoided. Using this technique, molecular ions derived from constrained rosettes, bis-stacked rosettes, and tris-stacked rosettes were directly observed. Only the least stable rosette aggregates that were poorly constrained failed to give rise to the predicted molecular ions. These two reports suggest that the use of electrospray mass spectrometry shows terrific promise for the characterization of small, weakly bound organic aggregates.

Reinhoudt and co-workers have combined the melamine−cyanuric acid motif with calix[4]arenes to make bis-stacked rosette assemblies with large cavities.[37] The keystone to this assembly is dimelamine-substituted calix[4]arene **2** which forms a molecular "box" when combined with barbiturate **3** (Figure 11). Notice that the calixarene provides the U-turn shape

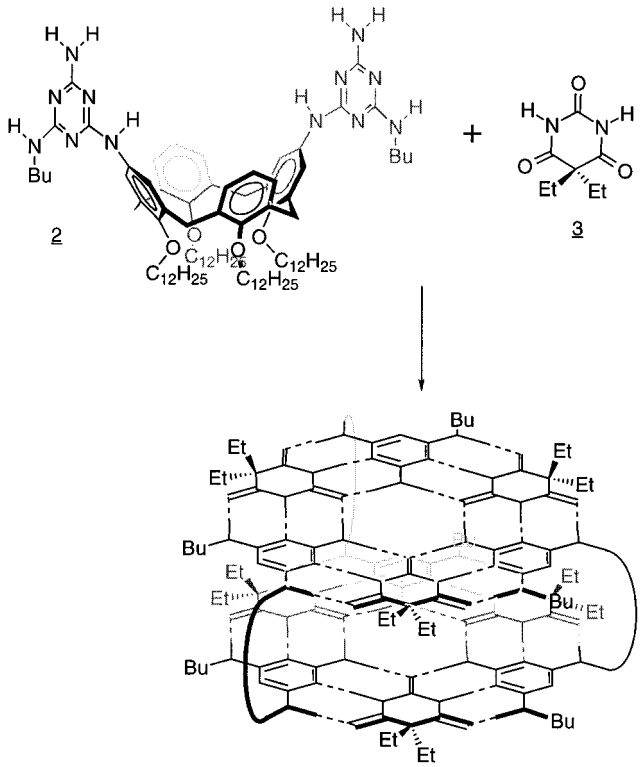

**Figure 11.** Assembly of a restrained bis-rosette structure.

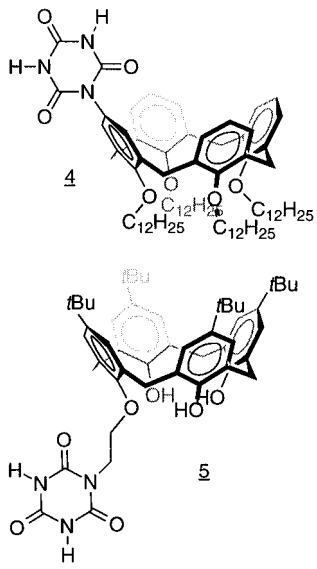

**Figure 12.** Substituted cyanuric acids.

which leads to the cavity, while the barbiturate acts as a "glue" to hold the box together. The evidence for the formation of this complex comes from $^1$H NMR studies in $CDCl_3$: at a 1:2 ratio of calixarene to barbiturate, the NMR spectrum is sharpened with respect to that of the starting materials and was concentration independent, although the range of concentrations explored was not specified; hydrogen-bonded melamine NH protons are shifted downfield; and additional equivalents of diethylbarbituric acid gave rise to a new set of signals, indicating slow exchange on the NMR time scale. Two-dimensional NOESY NMR experiments were used to estimate the distances between protons in the rosette and these values support the inferred structure. Initial growth rates of the nOe interactions were used to estimate the hydrodynamic volume of the rosette and this

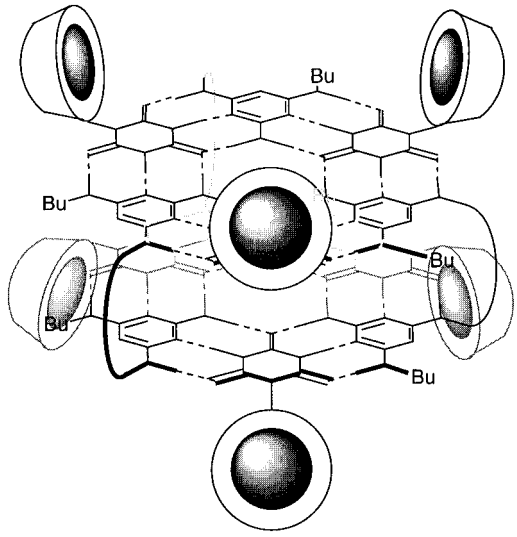

**Figure 13.** A schematic of the restrained bis-rosette with six pendant calix[4]arene groups.

value correlated roughly with the calculated values. It is unclear if this approach provides a more accurate estimate of molecular weight than other existing methods.

Calixarene-substituted cyanuric acids **4** and **5** (Figure 12) were also used in this motif, producing double rosettes with six pendant calixarene units. Because the gap between each rosette is only the width of a single calixarene, these additional macrocycles should not all face the interior of the cavity. Indeed, it is likely that they point toward the outer faces of the rosette box (Figure 13), although no efforts to clarify this were discussed. Although the complexation behavior of these double rosette boxes has not been reported, this motif has exciting possibilities toward this end. The space between the rosettes, predicted to be as much as 8.5 Å, should allow the complexation of large aromatic molecules and pendant calixarene units are excellent vessels for smaller aromatic molecules. A multiply bound double rosette box has potential as a molecular device capable of through-space energy or electron transfer.

## B. Macrocycle-Based Systems

### *1. Cyclodextrins*

Zhao and Luong have studied a simple self-assembling receptor based on the association of (hydroxypropyl)-$\beta$-cyclodextrin **6** and porphyrin tetracarboxylic acid **7** (Figure 14) through hydrogen bonding between the acids on the porphine ring and the hydroxyls on the upper rim of the cyclodextrins (Figure 15).[38] The association between the porphyrin and various cyclodextrins in water was monitored by both UV−vis and fluorescence spectroscopy, since conjugation of the carboxylate groups to the porphine ring causes large spectroscopic changes upon binding. The association process was also monitored by $^{13}$C NMR in water. Aggregation was found to be dependent upon the size and flexibility of the cyclodextrin ring. $\alpha$-Cyclodextrin, the cyclic hexamer of D-glucose, forms the weakest complex with the porphine ($K_d$ = 123 $\mu$M) while the complex with the cyclic glucose heptamer, $\beta$-cyclodextrin, is the strongest ($K_d$ = 14.2 $\mu$M). The octamer, $\gamma$-cyclodextrin, forms a somewhat weaker complex ($K_d$ = 19.2 $\mu$M). However, the hydroxypropyl derivative, **6**, by nature of its greater

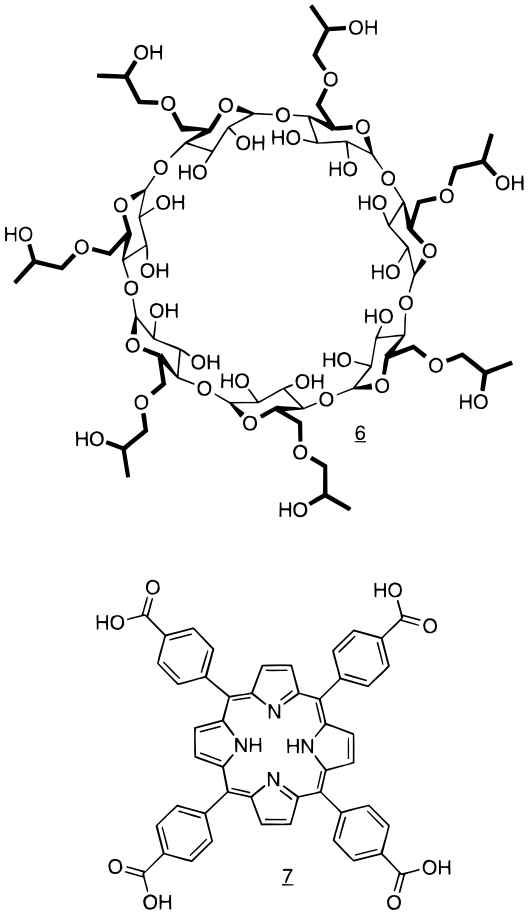

**Figure 14.** Cyclodextrin derivative **6** and porphine **7**.

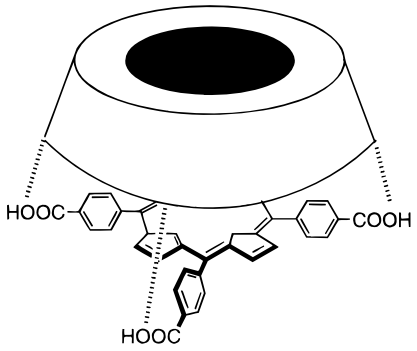

**Figure 15.** A schematic of the hydrogen-bonded complex formed between **6** and **7**.

flexibility, forms the strongest complex with a $K_d$ of 1.4 $\mu$M in water, as determined by UV-Vis titration.

This porphyrin−cyclodextrin aggregate was used as an aqueous sensor for pentachlorophenol, an environmental pollutant.[39] In the presence of pentachlorophenol, but not any other chlorinated phenol or chlorinated benzene, the characteristic 420.5 nm absorption maximum of the assembly shows a hypo- and bathochromic shift. Although all of the control molecules have high affinity for the assembly, only pentachlorophenol has a phenolic hydroxy group sufficiently acidic to change the absorption spectrum by hydrogen bonding to a nitrogen within the porphine ring.

### 2. Carcerands

Carcerands are typically covalently linked dimers of bowl-shaped macrocycles (Figure 16). Depending on the size and number of linkages between the

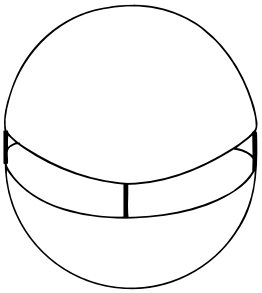

**Figure 16.** The generalized shape of a carcerand—two covalently connected hemispheres.

bowls, the carcerands can enclose a number of different guest molecules ranging in size from solvent molecules to hydrocarbons with formula weights over 200 Da, forming so-called carceplexes.[40] Passage of a guest into and out of the host requires heating to increase the opening of the portals, the mechanism of which has been explored computationally.[41,42] Because of the restricted access to the binding pocket, these carceplexes can be used to protect unstable intermediates from interaction with the outside environment. Among the tasks to which this strategy has been applied is the room-temperature stabilization of cyclobutadiene,[43] through-shell oxidation and reduction reactions,[44] nucleophilic substitution,[45] and through-shell triplet energy transfer.[46−48] The seminal contributions of Cram and co-workers have created an impressive taxonomy of carcerands and hemicarcerands, partially closed carcerands. Review of this field is presented in detail in an excellent book by Cram.[49]

Sherman and co-workers have described a template reaction where a small molecule guest, in *N*-methylpyrrolidin-2-one solvent, acts as a template to bring together two halves of a carcerand (Figure 17).[50] The resulting complex is then preorganized for the coupling reaction which subsequently forms the carceplex. The yield of the reaction corresponds to the templating ability of the guest, but not necessarily its affinity for the final carcerand. Further study by this group identified the complex as a dimer of semideprotonated tetrols with an enclosed guest (Figure 18).[51] Relative binding constants, determined by $^1$H NMR titration, confirm that pyrazine is the most strongly preferred guest over other small molecules (in decreasing order of binding: dioxane, DMSO, pyridine, benzene-$d_6$, acetone-$d_6$). There is a direct correlation between the ability of a molecule to act as a guest within this dimer and its ability to act as a template for the reaction. This suggests, indeed, that the tetraanionic dimer is involved in the template reaction.

### 3. Calix[4]arenes

Calixarenes, which are basket-shaped [1*n*] metacyclophanes most readily obtained by condensation of *p-tert*-butylphenol with formaldehyde, have long provided fertile ground for molecular recognition studies. The innate conformational flexibility of the calixarene (Figure 19) provides a versatile binding pocket for a number of different guest molecules ranging from metal ions to large aromatic molecules.[52−55]

Reinhoudt's group has exploited this motif to great end.[56] A self-assembling heterodimeric system was

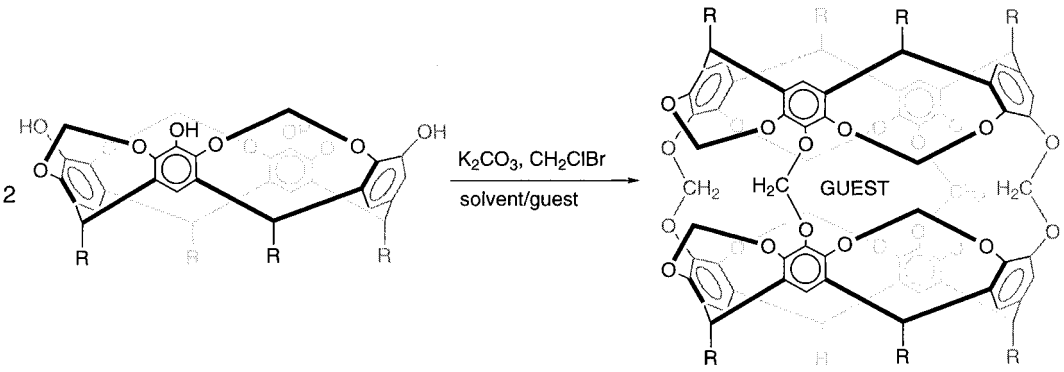


**Figure 17.** The template effect in carcerand formation.

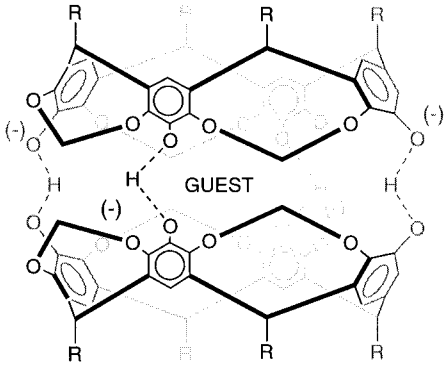


**Figure 18.** A noncovalently bound hemicarcerand dimer.

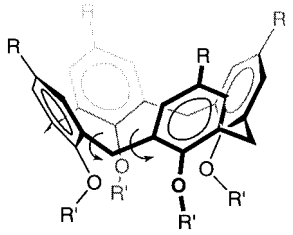

**Figure 19.** A generic calix[4]arene indicating rotatable bonds.

constructed exploiting the hydrogen-bond complementarity of pyridine and benzoic acid.[57] That is, calixarene **8**, tetrasubstituted at the bottom rim with the 4-pyridyl group, formed a one-to-one complex with calixarene **9**, modified with carboxylic acid groups at the upper rim (Figure 20). In $CDCl_3$, the dissociation constant is 132 $\mu$M. When the pyridine substituent was changed to 3-pyridyl, the geometry of the hydrogen bond was less favorable and the $K_d$ increased to 769 $\mu$M. When the substituent was changed to 2-pyridyl, no association was observed. $^1$H NMR dilution studies confirmed that the association is based upon hydrogen bonding rather than electrostatic interactions resulting from proton transfer. The IR spectrum of a 1:1 complex showed a broad signal at 1942 cm$^{-1}$, corresponding to pyridine-bound OH groups, but no change in the carbonyl stretching frequency, indicating that no substantial proton transfer occurred. Vapor-pressure osmometry studies further corroborated that the two calixarenes formed a discrete 1:1 aggregate. The measured molecular weight agreed well with the expected value (2004 ± 200 vs 2263 g/mol). The ability of this aggregate to complex guest molecules has not yet been examined.

A similar system constructed by Shinkai and coworkers features two calixarene subunits function-

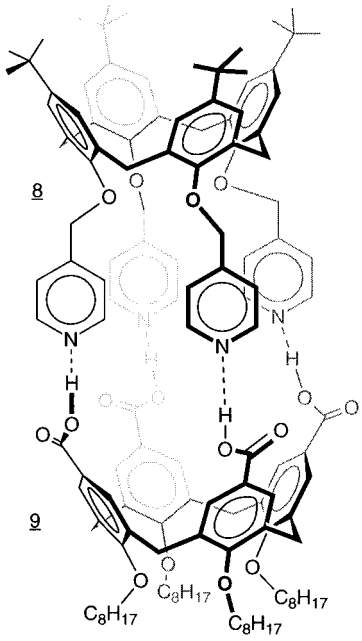


**Figure 20.** Hydrogen bonding between lower-rim/upper-rim-substituted calixarenes.

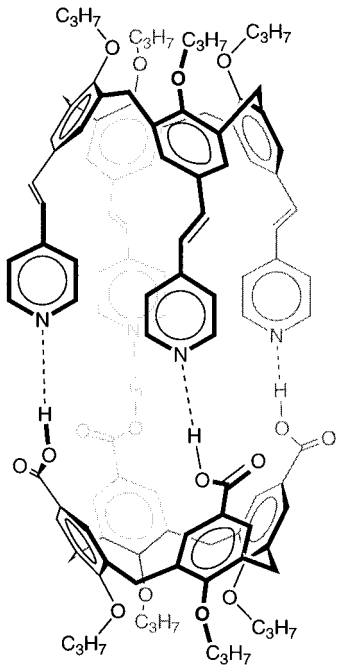

**Figure 21.** Hydrogen-bonding between upper-rim/upper-rim-substituted calixarenes.

alized at the upper rim (Figure 21).[58] The formation and stoichiometry of a 1:1 complex was confirmed by

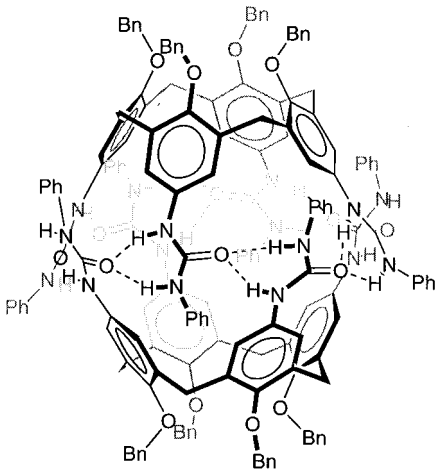

**Figure 22.** The dimeric form of tetraarylurea-substituted calix[4]arene.

vapor-pressure osmometry and concentration-dependent fluorescence spectroscopy. No change in the $^1$H NMR spectrum was observed nor were association constants reported.

Rebek and co-workers reported a top-rim derivatized calixarene which dimerizes to form a capsule capable of binding small molecules by inclusion.[59,60] The overall architecture of the assembly resembles two hemispheres "zippered" together along the equator by hydrogen-bonded ureas (Figure 22). This hydrogen-bonding pattern of ureas has been well established, particularly in the solid state,[61] where X-ray crystallography has shown that the head-to-tail arrangement is a common geometry. All eight ureas may be fixed in same direction forming up to 16 hydrogen bonds. The hydrogen-bonding slows rotation about the calixarene-urea bond resulting in an isomer of $D_{4d}$ symmetry.

Evidence for assembly formation in solution was derived from $^1$H NMR spectroscopy and plasma desorption mass spectrometry where a molecular ion peak corresponding to ($M^+$ plus included solvent), dependent on the last solvent used, could be seen.[59] Additional evidence for the existence of the tetraurea−calixarene as a hydrogen-bonded dimer in nonpolar solvents came from the encapsulation of solvent molecules inside the assembled cavity.[59,60] Inclusion was initially apparent in mixed-solvent systems where two distinct calixarene assemblies were observed by $^1$H NMR. Direct observation of the encapsulated guests by $^1$H NMR was also possible, given some time. The interleaved geometry of the assembly prevents visiting guests from leaving or entering quickly. Although no equilibrium constant was determined for the aggregation process, it is favored enough to overcome the flexibility of conformationally unrestrained calixarenes.[62] When the lower rim substituents are methyl groups, a calixarene can exist in a mixture of cone and partial cone conformations. By virtue of the aggregation process, however, the tetraurea calixarenes exist solely in the cone conformation. This can also be considered as additional evidence for the dimeric state.

This self-assembled dimer was capable of encapsulating a single molecule with a preference for molecules no larger than benzene.[60] For instance, the best guests for this receptor, with relative dissociation constants as determined in *p*-xylene-$d_{10}$ shown

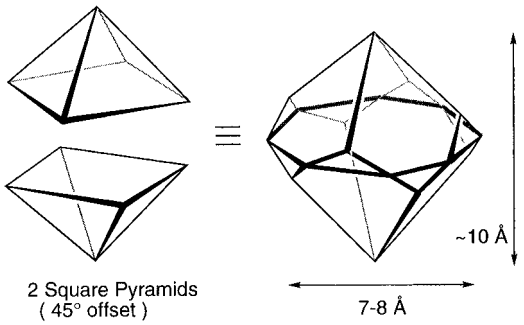


**Figure 23.** A schematic of the geometry of the calixarene dimer showing approximate dimensions as measured by molecular modeling.

in brackets, are benzene (1.0), pyridine (1.2), fluorobenzene (2.6), pyrazine (3.2), and *p*-difluorobenzene (5.8). In contrast, larger benzene derivatives such as chlorobenzene, toluene, and aniline all showed a reduced affinity for this cavity. The length of the guest appears to be crucial for its ability to bind within the cavity. For instance, *p*-xylene is a poorer guest than *o*-xylene despite the fact that they have much the same molecular volume. $^1$H NMR evidence from the complex with fluorobenzene was given suggesting that the encapsulated arenes are positioned perpendicularly to the long axis of the capsule. That is, electronegative substituents, like fluorine, and the *para* hydrogen point at the belt of ureas while the *ortho* and *meta* hydrogens face the aromatic rings of the calixarene. This geometry would also be expected for the binding of pyrazine within the dimeric host. The calixarene dimer can be schematically represented as a gem-like geometry with an octagonally shaped horizontal cross section and a diamond-shaped vertical cross section (Figure 23). On the basis of this model, Rebek and co-workers predicted that cubane could be enclosed by the calixarene dimer and observed this complex in *p*-xylene-$d_{10}$, although no association constant was determined. The association of the dimer can be disrupted by addition of other ureas, which likely interfere with dimerization by competitive hydrogen bonding.

Böhmer and co-workers independently also studied the same system.[63] In addition to stereochemical evidence for dimerization from the $^1$H NMR spectrum (the dimer has $S_8$ symmetry and the $OCH_2$ protons are diastereotopic), these workers exploited heterodimerization to provide additional proof of the dimeric structure. That is, when two different tetraureas (*e.g.*, Figure 24, R = Bu and R′ = Ph) were mixed in apolar solvents such as $CDCl_3$ or $C_6D_6$, the $^1$H NMR spectrum showed three species in solution—the two homodimers and another set of peaks assigned as the heterodimer. Earlier indications suggested that the aggregation process is statistical. When this experiment was performed in a competitive polar solvent (DMSO-$d_6$), where hydrogen bonding is disrupted, only two pure compounds were observed. Recently, this group has also directly observed the dimeric structure of these urea−calixarene assemblies by X-ray crystallography.[64]

Reinhoudt and co-workers have studied a similar aggregate.[65] In this case, only two of the phenyl subunits were substituted with urea functionality. This disubstituted calixarene was found to have restricted conformational flexibility in nonpolar or-

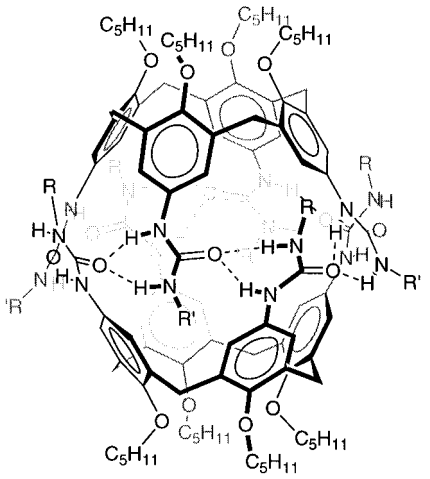

**Figure 24.** The tetraarylurea-substituted calix[4]arene *hetero*dimer.

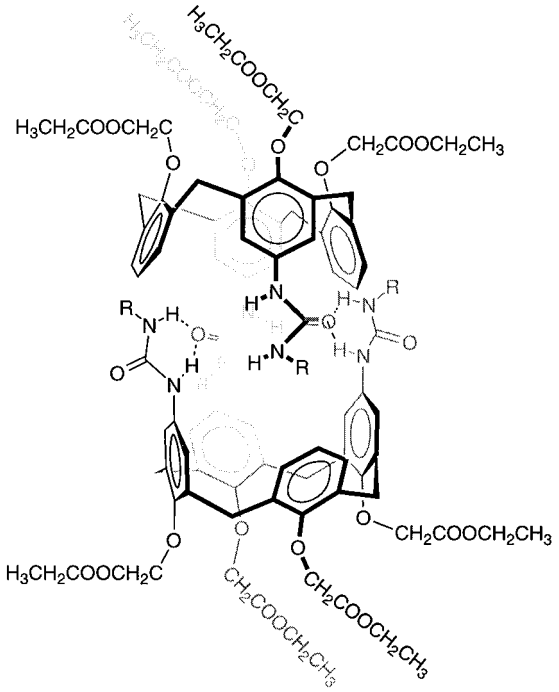

**Figure 25.** Dimerization of diarylurea-substituted calix-[4]arene.

ganic solvents by virtue of intramolecular hydrogen bonds between the urea functionalities. With appropriate substituents on the urea (Figure 25, R = phenyl, *tert*-butyl), the calixarene dimerized as determined by concentration-dependent FT-IR measurements and observation of intermolecular nOe connectivities by $^1$H NMR. Dimerization was not observed when the urea substituent was instead *n*-octyl. This work did not discuss the ability of this assembly to bind small molecule guests, but undoubtedly this work is forthcoming.

### *4. Resorcinol Cyclic Tetramer*

In nonpolar organic solvents, the resorcinol cyclic tetramer (Figure 26) binds methyl glucopyranoside via hydrogen bonding.[66] The complex was predicted to have a single methyl glucoside bound within a cavity formed by two resorcinol tetramers (Figure 27). This prediction was based on solid−liquid extraction studies (methyl glucoside is ordinarily insoluble in the solvents used) and on $^1$H NMR studies of the

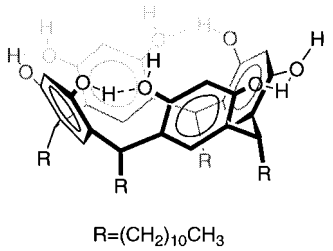

**Figure 26.** The resorcinol cyclic tetramer.

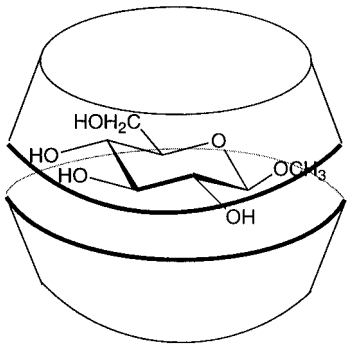

**Figure 27.** Complexation of $\beta$-methyl glucoside by a dimer of the resorcinol cyclic tetramer.

complex in $CDCl_3$. The molecular weight of the complex was determined by means of vapor-pressure osmometry. Complexation was confirmed by reextraction of the glucoside into water, where it was examined by $^1$H NMR to confirm that the compound was unchanged, and by circular dichroism studies. The achiral, chromophoric host showed an induced circular dichroism spectrum upon interaction with the chiral, nonchromophoric guest, methyl glucoside. This complexation phenomenon was specific for the $\beta$-anomer, over the $\alpha$-anomer. Because of the heterogeneous nature of the extraction studies, affinities were not determined.

## C. Glycouril-Based Systems

### *1. Cucurbituril*

Cucurbituril is a rigid cyclic glycouril hexamer (Figure 28) with a central hollow core of diameter 5.5 Å. The upper and lower rims of the macrocycle are lined with inwardly pointing carbonyl groups. By virtue of strong electrostatic interactions, cucurbituril is capable of binding strongly to aliphatic and aromatic ammonium ions.[67] Kim and co-workers have recently observed that cucurbituril, normally water insoluble except in strongly acidic solutions, can be solubilized by alkali metal salts (0.2 M).[68] X-ray analysis of crystals of cucurbituril grown from aqueous sodium sulfate show that sodium ions provide a "lid" on both the top and bottom of the macrocycle.

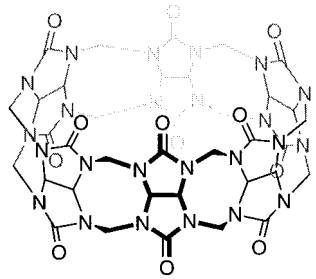

**Figure 28.** Cucurbituril.

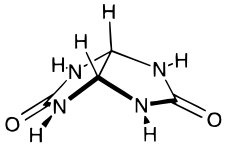

**Figure 29.** Glycouril.

Two sodium ions and five water molecules form a network of hydrogen bonds and electrostatic interactions between the six carbonyl groups. This network restricts access to the interior of the macrocycle and under these conditions cucurbituril was able to bind to a number of small organic molecules. As determined by relative integration of bound and unbound guest peaks in the $^1$H NMR spectra, the dissociation constants are THF, $K_d$ = 2.0 mM; benzene, $K_d$ = 37 mM; cyclopentanone, $K_d$ = 455 $\mu$M; and furan, $K_d$ = 140 $\mu$M. The crystal structure of the THF-bound cucurbituril showed the that guest was disordered over two sites with no apparent specific interactions between the oxygen of THF and the sodium ions in the "lids". Although the network structure was the same in both the THF- and water-included structures, $^{23}$Na NMR studies indicated that the coordinated sodium ions were in rapid exchange. The inclusion of THF inside the sodium-lidded cucurbituril is enthalpically favored ($\Delta H° = -5.8$ kcal/mol) and entropically disfavored ($\Delta S° = -7.4$ cal/K·mol). The implication of this study is that in strongly acidic solutions, cucurbituril is lidded by a hydrogen-bonded network of water molecules and hydronium ions, which is insufficient to restrain uncharged guests within the cavity. Kim and co-workers exploited this observation to regulate inclusion by changing pH. To be specific, lowering the pH of solution by addition of TFA caused release of bound THF, as determined by $^1$H NMR spectroscopy. Addition of sodium carbonate caused the reencapsulation of THF.

### *2. Seamed Spheres*

Two features of the glycouril group make it an ideal structural unit for the construction of self-assembling molecules—its intrinsic curvature and multiple hydrogen-bonding groups (Figure 29). The Rebek group has studied a series of self-assembling capsules based upon the dimerization of glycouril derivatives.

*a. "Tennis Balls" and "Baseballs".* The first assembly in this series consisted simply of two diphenylglycouril units linked by a durene spacer (Figure 30).[69] The dimerization proposal was supported by $^1$H NMR studies in both $CDCl_3$ and benzene-$d_6$ where only one species was observed and the NH protons were significantly shifted downfield; mass spectrometry where a peak corresponding to the dimer was observed by EI-MS, FAB-MS, MALDI-MS, and vapor pressure osmometry. The structure of the dimer was predicted on the basis of molecular modeling[70] and was recently confirmed in the solid state by X-ray crystallography (Figure 31).[71] The assembly is held together by eight almost linear (167−178°) hydrogen bonds with N−O distances of 2.78−2.89 Å.

The expectation that the simple dimer could encapsulate small molecules was confirmed by $^1$H NMR studies where upfield signals for included guests were observed.[72] For example, when methane was added to a solution of the assembly in $CDCl_3$, a peak corresponding to bound $CH_4$ arose at −0.91 vs 0.23 ppm for free methane (unlike all other encapsulated guests, the $^{19}$F NMR signal corresponding to bound $CF_4$ was found *downfield* from the signal of free $CF_4$[73]). Dissociation constants at 0 °C were determined by relative integration of free and bound guest signals for $CHCl_3$ (25 M), $CF_4$ (357 mM), $CH_2Cl_2$ (250 mM), $H_2C{=}CH_2$ (3.6 mM), and $CH_4$ (3.3 mM).[72,73] Temperature-dependent $^1$H NMR studies were used to determine the enthalpy and entropy of the encapsulation process. In all cases, entrapment was disfavored entropically by some 20−45 cal/K·mol but was compensated by favorable enthalpy. A crude inverse correlation between binding affinity and guest volume could be drawn, although free energy perturbation calculations performed by Kollman and co-workers have a somewhat more solid theoretical grounding.[74] While the relative affinities of chloroform, tetrafluoromethane, and methane were qualitatively justified by the calculations, quantitation of the energy factors should still be considered crude.

Although the initial studies were performed in nonpolar solvent, assembly of the dimer was also observed in the more competitive polar solvent, DMF-$d_7$, as a result of nucleation.[75] Good guests such as methane, ethylene, argon, or xenon are effective nucleators; hydrogen, helium, and neon are not. The encapsulated xenon atom was observed by $^{129}$Xe NMR and displayed an upfield chemical shift. These studies were performed using a derivative of the original tennis ball with dimethylaniline substituents (Figure 32). The presence of this basic functionality allowed control of the aggregation process by adjusting the acidity of the medium. When a large excess (~80 equiv) of *p*-TsOH was added, the aggregate completely disassembled, presumably by the excess of charge around the periphery of the molecule, although the exact sites of protonation were not determined. This process is reversible and addition of sodium carbonate regenerated the xenon-included dimer.

The versatility of the glycouril "tennis ball" motif was further demonstrated in a recent paper.[73] Utilizing a dihydroxylated central benzene spacer, García and Rebek constructed two new aggregates with

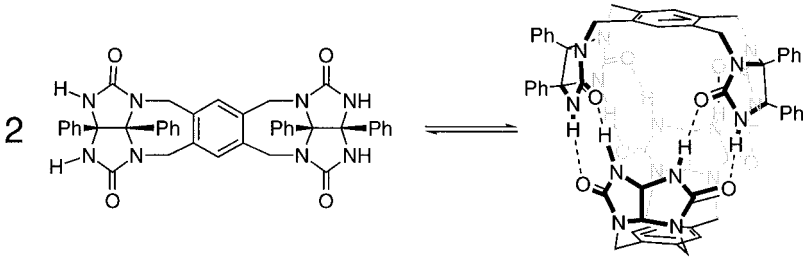

**Figure 30.** Dimerization of a bis(glycouril)macrocycle by hydrogen bonding.

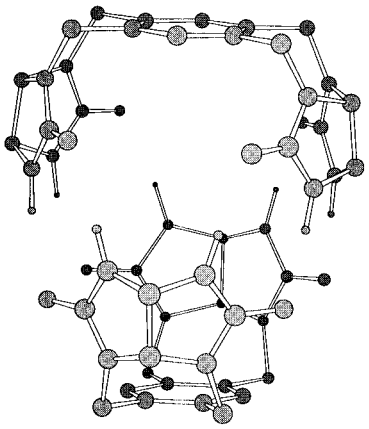

**Figure 31.** The crystal structure of the "tennis ball". Hydrogens attached to carbon and glycouril substituents have been omitted for clarity.

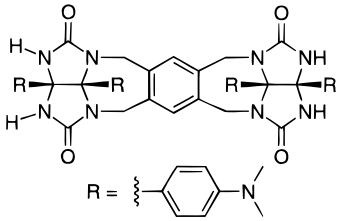

**Figure 32.** Acid-controlled assembly with dimethylaniline substituents.

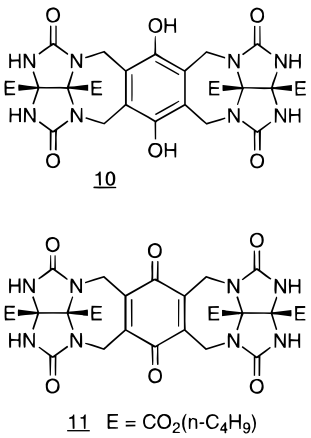

**Figure 33.** Hydroxy substitution allows control of the electronic nature of the binding cavity.

altered electronic properties in the cavity (Figure 33). As determined by now-standard NMR studies at room temperature, the hydroquinone assembly (**10**) was a better receptor than the unsubstituted derivative while the quinone derivative (**11**) was not as effective. For instance, methane had dissociation constants of 30, 14, and 100 mM for the unsubstituted, hydroquinone, and quinone assemblies, respectively. Circumstantial evidence for the encapsulation of nitric oxide was given: oxidation of hydroquinone **10** to the quinone **11** with $NO_2$ gave a solid product after evaporation of volatiles. This product spontaneously oxidized another equivalent of **10** assembly when redissolved. Identification of the active oxidant—either included NO or $O_2$ (catalyzed by residual nitrogen oxides)—is ongoing.

Because **10** and **11** have the same shape, the formation of heterodimers is facile, as determined by NMR spectroscopy. Rebek and co-workers have expanded the library of assemblies by varying the

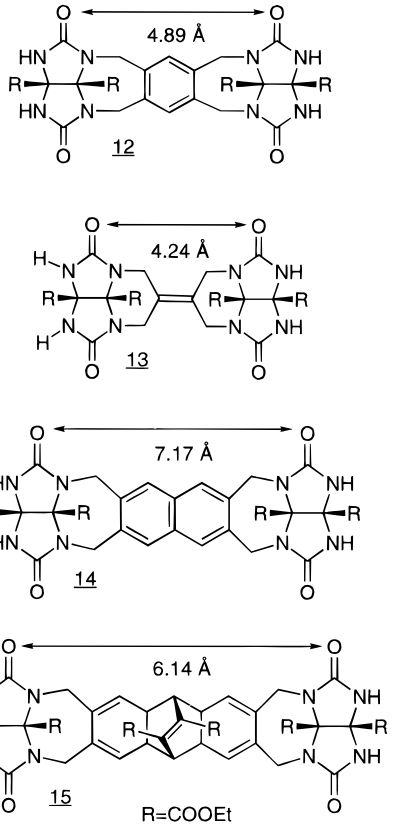

**Figure 34.** Variation of carbonyl−carbonyl spacing with changing spacer length and bending.

size of the intervening spacer.[71] Figure 34 shows the original molecule and three variants along with the carbonyl−carbonyl separation predicted by molecular modeling. The dimer **13**−**13** behaved normally but, with a cavity much smaller than **12**−**12**, it bound methane more poorly ($K_d$ = 238 mM at 0 °C) and did not bind ethane all. The enlarged spacing of the naphthyl unit of **14** was predicted to preclude efficient dimerization. No bound guest was observed by NMR and the dynamic nature of the spectra prevented evaluation of the efficiency of dimerization. The curvature of **15** brings the carbonyl groups closer together and this structure was predicted to dimerize efficiently. Unfortunately, rapid exchange on the NMR time scale (presumably because of the large 'pore" size) prevented observation of bound molecules, although the $^1$H NMR spectrum of the molecule itself showed some visible changes with the proportion of added $CDCl_3$, a good guest for the cavity. The predicted geometries of all three homodimers are shown in Figure 35.

Recombination of these molecules produced heterodimers with new capsule shapes.[71] Molecular modeling was used to predict which heterodimeric combinations were likely to form: hybrid structures **12·13**, **12·15**, and **14·15**. The energy-minimized structures of the heterodimers are shown in Figure 36. When two different dimers were present in the same solution, a new species, the heterodimer, was also observed by $^1$H NMR. Again, indirect evidence for the capsule-like nature of the new species was taken from the observation of a new NMR signal for enclosed solvent.

The recombinations (disproportionation equilibria) of the dimers depended strongly on the solvent,

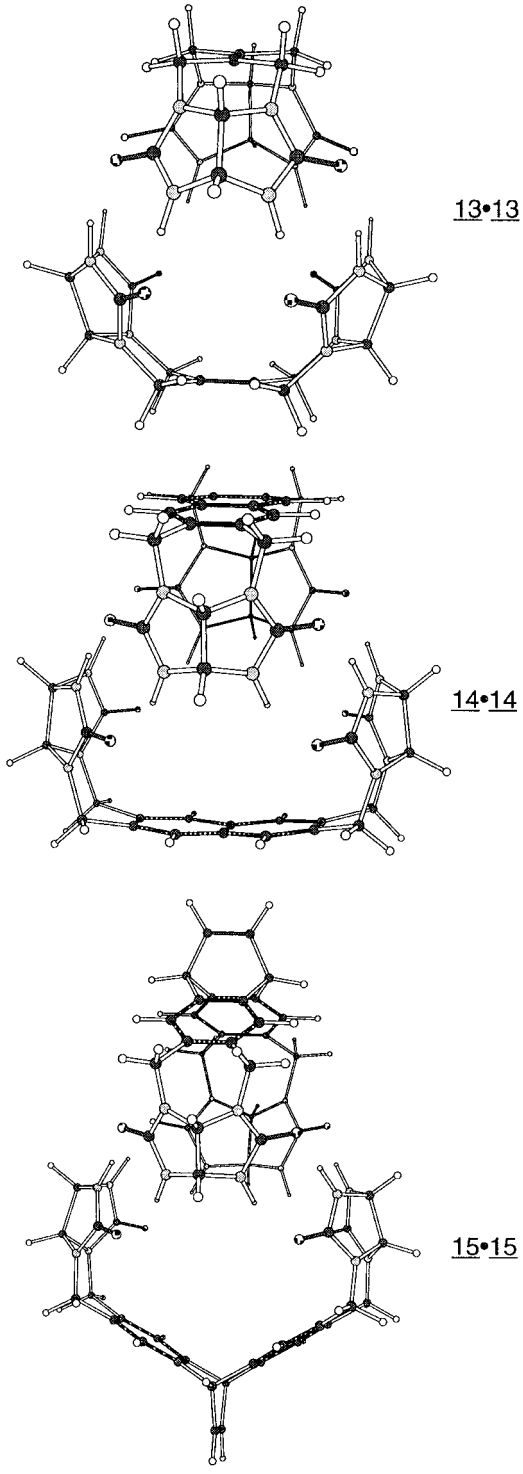


**Figure 35.** Predicted structures of homodimeric capsules. Hydrogens attached to carbon and glycouril substituents have been omitted for clarity.

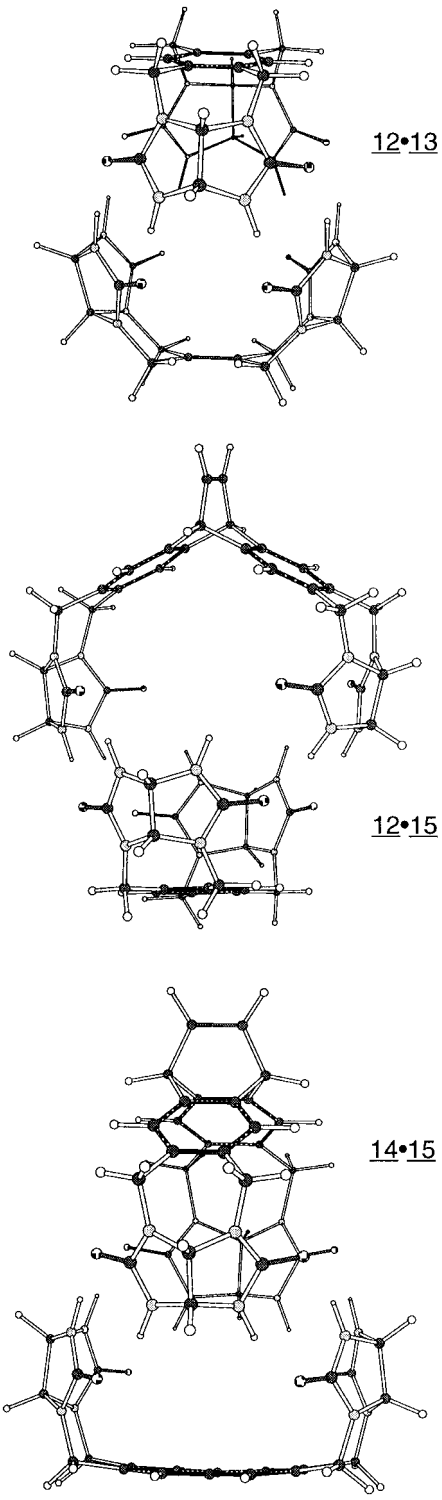


**Figure 36.** Predicted structures of heterodimeric capsules. Hydrogens attached to carbon and glycouril substituents have been omitted for clarity.

although all three heterodimers followed the same order: $CD_2Cl_2 < CDCl_2CDCl_2 < CDCl_3 < CDBr_3$. The enthalpy and entropy of the disproportion were determined in $CDCl_3$. However no clear trend was observed: the **12**−**13** and **14**−**15** heterodimerization processes were favored enthalpically and disfavored entropically while the formation of **12**−**15** was enthalpically disfavored and entropically favored.

*b. "Softballs".* In an effort to develop self-assembling dimers capable of recognizing and binding larger molecules, Rebek and co-workers further expanded the size of the spacer between the two glycouril units while still keeping an appropriate

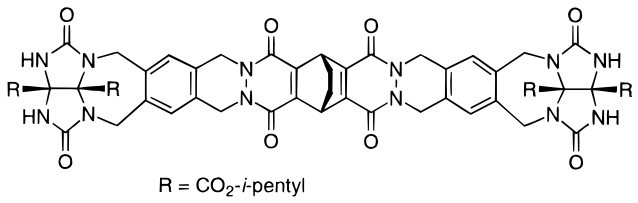


**Figure 37.** Larger assemblies are possible with the "softball".

shape to allow dimerization to occur (Figure 37).[76] Evidence for the formation of a dimer was drawn

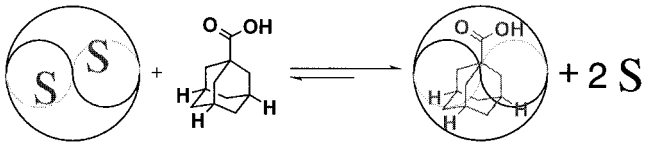

**Figure 38.** Complexation is an entropy-driven process due to the release of multiple solvent molecules into the bulk phase.

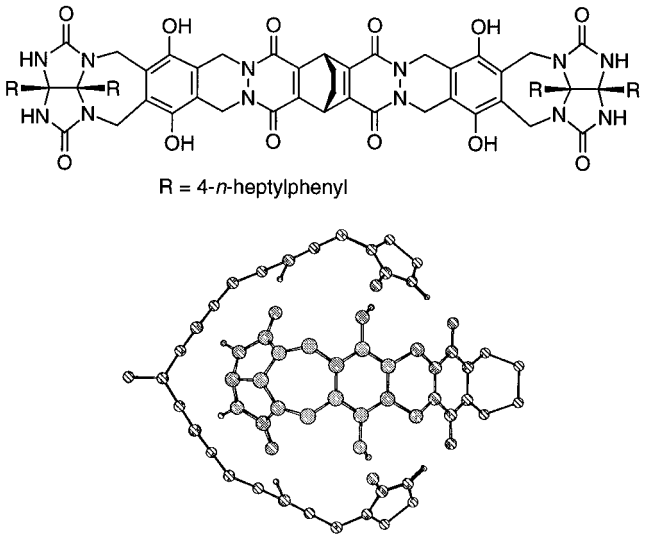


**Figure 39.** Structure and predicted fold of the "zippered" softball.

from $^1$H NMR chemical shifts in benzene-$d_6$, which acts as a guest within the capsule. In *p*-xylene-$d_{10}$, a poor guest for the cavity, the $^1$H NMR spectrum was broad, indicating extensive nonspecific aggregation but the addition of medium-sized molecules caused formation of a single dimeric capsule. The best guests for the capsule were 1-adamantanecarboxylic acid ($K_d$ = 1.3 mM) and 1-ferrocenecarboxylic acid ($K_d$ = 3.6 mM). With this new shape, the guest molecules are of a more practical size and the binding affinities are improved. A study of the thermodynamics of the encapsulation process revealed that the encapsulation of 1-adamantane carboxamide, to be specific, increased with increasing temperature.[77] That is, in toluene-$d_8$ the process is entropy driven: $\Delta H$ = 7.3 kcal/mol, $\Delta S$ = 35 cal/K·mol. The explanation for this resides with encapsulated solvent. Two solvent molecules bound within the capsule are released when a single guest molecule binds within the cavity (Figure 38). This entropic driving force is more commonly seen in aqueous solvents, where it appears as the hydrophobic effect. Further evidence in support of this hypothesis came from studies using mixed solvent systems where three different assemblies were observed by $^1$H NMR—capsules which contained two molecules of benzene-$d_6$, two molecules of fluorobenzene-$d_5$, or one molecule of each.

A further improvement on this "softball" design is shown in Figure 39.[78] The addition of phenolic groups creates the possibility for an additional eight hydrogen bonds in the dimeric assembly. This favors dimerization even further over other aggregates. The most favored guests were similarly sized as before, but the more robust dimer showed much greater affinities (10−20-fold lower dissociation constants). In $CDCl_3$, 1-adamantanecarboxylic acid ($K_d$ = 179 $\mu$M) and 1-ferrocenecarboxylic acid ($K_d$ = 59 $\mu$M)

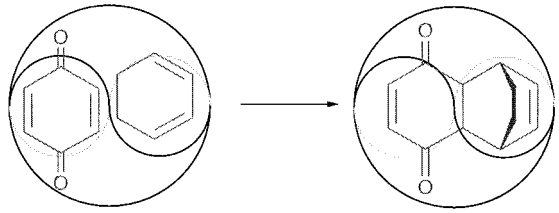

**Figure 40.** Diels−Alder reaction can take place within the assembled cavity (schematic).

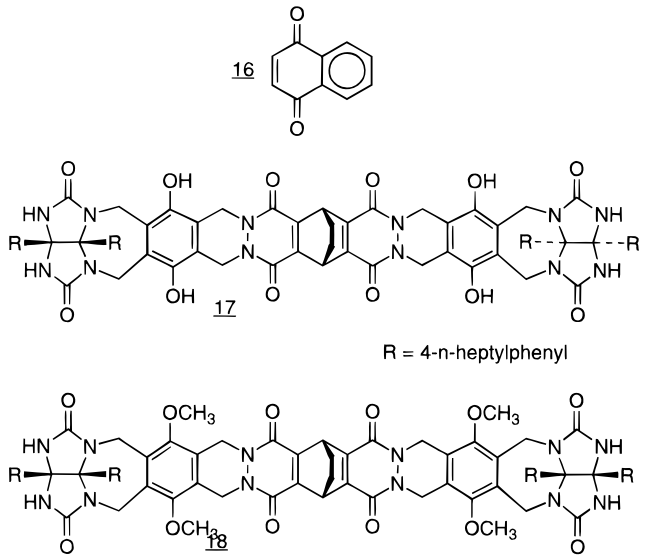


**Figure 41.** Control molecules. Oversize substrate (**16**), A nonassembling C-shaped molecule (**17**), and a neutered half shell (**18**).

remain favorite guests. Thematically, exchange is slow on the NMR time scale and association constants were determined by integration of peaks from bound and unbound guest. Examination of the thermodynamics of encapsulation revealed that the binding of guests by this capsule is also entropically driven. With a capsule capable of high binding affinity for multiple small guests, Kang and Rebek have demonstrated the ability of this hydrogen-bonded aggregate to act as a "reaction chamber" to accelerate a Diels−Alder reaction (Figure 40).[79] When both *p*-quinone and cyclohexadiene were present in solution, a single well-defined complex was observed in the NMR spectrum. Integration showed more than one molecule of quinone was present within this complex with two captive quinones being the predominant species, but no signals unique to encapsulated cyclohexadiene could be assigned. Nonetheless the encapsulated Diels−Alder adduct was observed by NMR within one day. The half-life for the reaction in bulk solution at the concentrations used in this experiment is on the order of a year. Unfortunately, this system is plagued by severe product inhibition, so no turnover could be observed (the $K_d$ for the product is less than 10 $\mu$M). On the basis of the initial rates, the effective molarity (EM) of the reactants inside the chamber was estimated to be 2 M. Saturation kinetics were observed with regard to cyclohexadiene concentration with a $k_{cat}$ of 1/day, a 200-fold rate acceleration. Three control molecules were employed to test if another mechanism aside from encapsulation was responsible for the observed rate acceleration (Figure 41). First, a larger dienophile **16**, incapable of binding within the capsule, was

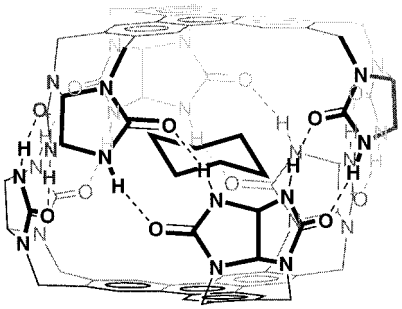

**Figure 42.** A cyclohexane-filled "jelly doughnut".

used in the reaction. No catalysis was observed. Secondly, an S- rather than C-shaped derivative of the self-assembling molecule (**17**) was found to be inactive and, thirdly, the S-shaped alkylated derivative **18** was also found to be inactive. These two controls show that neither the shape, nor functionality of the capsule alone is sufficient for catalysis; both must be present (*i.e.* encapsulation must occur for catalysis).

### *3. Flattened Spheres*

The complexity of glycouril assemblies was increased by using a triphenylene scaffold to allow three glycouril groups to interact. The resulting assembly has $D_{3d}$ symmetry and was described as having the appearance of a "jelly(-filled) doughnut" (Figure 42).[80] The ceiling and floor of the assembled capsule consist of aromatic $\pi$-surfaces; 12 strong hydrogen bonds hold the two halves together. Similar to the previous assemblies, this dimeric structure was capable of encapsulating small molecules. The evidence for this encapsulation was taken from $^1$H NMR and $^{13}$C NMR studies where upfield signals corresponding to enclosed guest, which are in slow exchange with free guest, were observed. This cavity was demonstrated to have preferential affinity for disk-shaped guests with a narrow size limit. As determined by titration of the solvated assembly with a new guest molecule, benzene replaced $CDCl_3$ and cyclohexane completely displaced *p*-xylene-$d_{10}$. Equilibrium constants for these two processes were not determined. While the exchange rate between encapsulated $CDCl_3$ and benzene was rapid, the half-life of exchange of cyclohexane in *p*-xylene-$d_{10}$ solution was observed to be on the order of 2.5 h. It was suggested that the slow rate of exchange was due to the requirement that a number of hydrogen bonds must be broken before this larger guest could pass into and out of the cavity.

## D. Base Pairing

The hydrogen bonding between DNA bases has long been a favorite vehicle for studies in molecular recognition.[81−92] It seems only fitting, then, that these interactions form the basis for self-assembling receptors.

Schall and Gokel have reported a bis-crown ether aggregate whose formation is driven by base pairing.[93] By tethering the bases adenine or thymine to 4,13-diaza-18-crown-6, a self-assembling receptor for dialkylammonium ions was generated (Figure 43). Due to the unconstrained nature of the construct, both intra- and intermolecular interactions prevail.

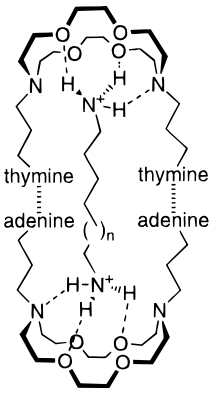


**Figure 43.** A base-paired self-assembling dialkylammonium receptor.

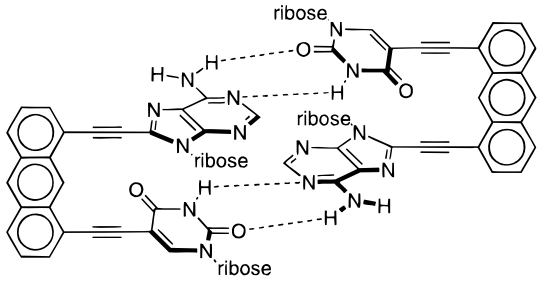


**Figure 44.** Greater rigidity improves the assembly of an artificial dinucleotide.

Furthermore, the nature of the hydrogen-bonding interaction between the subunits appeared to diverge somewhat from the canonical base-pair motif. Nonetheless, the adenine−crown−adenine and thymine−crown−thymine subunits assemble in $CDCl_3$ with a dissociation constant of 1.1 mM, as determined by $^1$H NMR titration. Additional support for the dimeric structure came from vapor-pressure osmometry studies which indicated an average molecular weight approaching, but not quite, that of the heterodimeric species. The aggregate was able to bind alkyldiammonium salts (decyl and dodecyl), but solubility and conformational complications prevented the determination of equilibrium constants.

Sessler and Wang have recently constructed an "artificial dinucleotide duplex" which features considerably greater conformational control.[94] Adenine and thymine were connected to anthracene by rigid acetylene units (Figure 44). In $CDCl_3$, the dimeric aggregate was observed directly by $^1$H NMR. Titration of the solution with DMSO-$d_6$ to 60% (v/v) disrupted the aggregate completely, but at 45% (v/v) DMSO-$d_6$/$CDCl_3$ a dissociation constant of 29 mM could be determined by relative integration of the dimeric and monomeric signals, which are in slow exchange with one another. The dimerization was further supported by FAB-MS studies where a molecular ion peak attributable to the dimer was observed and vapor-pressure osmometry measurement in 1,2-dichloroethane. Preliminary evidence for the binding of two molecules of solvent was derived from elemental analysis. Peaks corresponding to two molecules of solvent were also observed by $^1$H NMR spectroscopy of material recrystallized from dichloroethane. At this stage, no distinction was made between binding within the confines of the assembly or in the form of a clathrate. We eagerly await the latest word on this system.


$B_{10}C_2H_{12}$

**Figure 45.** 1,2-Dicarbadodecaborane.

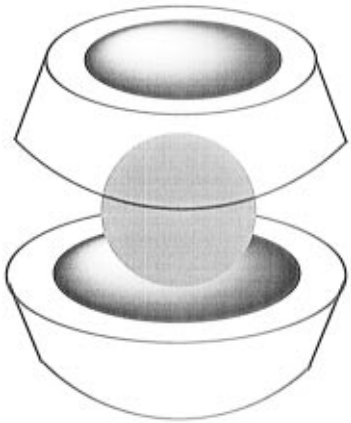

**Figure 46.** Proposed structure for the 2:1 α-cyclodextrin: carborane complex.

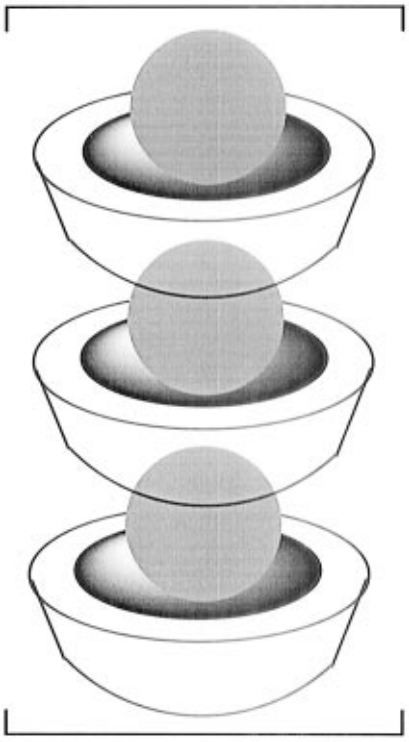

**Figure 47.** Proposed infinite array structure for the 1:1 α-cyclodextrin:carborane complex.

## III. Hydrophobic Assemblies

The natural concavity of cyclodextrins and cyclophanes has been exploited in the formation of capsule complexes. These macrocycles, by nature of their hydrophobic interiors, sequester nonpolar molecules from aqueous solution. Generally speaking, these are phenomena that are observed, rather than designed. In principle, any hydrophobic moiety larger than a single cyclodextrin cavity is capable of templating a 2:1 cyclodextrin:guest complex.

Although their assemblies were studied only in the crystalline state, Harada and Takahashi prepared inclusion complexes of α-, *β*-, and *γ*-cyclodextrin (cyclic hexamer, heptamer and octamer, respectively, of glucose) and 1,2-dicarbadodecaborane (*o*-carborane, Figure 45).[95] While the larger cyclodextrins formed a 1:1 inclusion complex with the carborane in aqueous solution, α-cyclodextrin is too small to completely enclose the substrate. When solid *o*-carborane was sonicated in a saturated aqueous solution of α-cyclodextrin, crystalline complexes of two cyclodextrins and one carborane were isolated. However, when an alcoholic solution of *o*-carborane was added to aqueous α-cyclodextrin, a 1:1 complex precipitated from solution. The preparations were characterized by elemental analysis, IR spectroscopy and $^1$H NMR spectroscopy. On the basis of the stoichiometry of the two different preparations, Harada and Takahashi proposed a capsule-like geometry for the 2:1 complex (Figure 46) and an infinite stacked tube for the 1:1 complex (Figure 47).

Davies has undertaken detailed studies on the binding of substituents into the α-cyclodextrin cavity.[96] In particular, a series of para-disubstituted aryl alkyl sulfides, sulfoxides, and sulfones were studied. As determined by UV titrations in aqueous solution, the sulfides, but not the sulfoxides or sulfones, were observed to favor the formation of a 2:1 cyclodextrin: sulfide complex. Methyl *p*-tolyl sulfide was found to favor this aggregation most strongly with a dissociation constant of 1 mM from the 2:1 complex and a dissociation constant of the 1:1 complex of 24 mM.

The hydrophobic effect is also responsible for the capture of buckminsterfullerene ($C_{60}$) from aqueous suspensions by *γ*-cyclodextrin. The proposed structure of the complex is of the same form as shown in Figure 46 for the cyclodextrin−carborane complex. The $C_{60}$:*γ*-cyclodextrin inclusion complex can be simply prepared, although the stability of the resultant complex varies depending on the method of preparation.[97−99] Since the first report of water-solubilized $C_{60}$ in 1992, over 60 articles have appeared studying its unusual structural, spectroscopic, and electronic properties. The interested reader is referred to a review in *Comprehensive Supramolecular Chemistry*[100] and recent computational studies examining the process through which symmetrical $C_{60}$ is encapsulated by two unsymmetrical *γ*-cyclodextrin molecules.[101−103]

Pyrene induces the formation of a 2:1 cyclodextrin aggregate in aqueous solution, also of the same form as Figure 46.[104] In this case, Muñoz de la Peña and co-workers determined that alcohols added to the solution affect the stability of the 2:1 complex and that the structure of the alcohol is important. Using fluorescence titrations, they determined that the pyrenealcohol ratio is 1:2, which implies that the stoichiometry of the aggregate in aqueous solution is 2:1:2 cyclodextrinpyrenealcohol. Inclusion is favored by branched alcohols. The best guest was cyclopentanol ($K_d$ = 1 nM). From this, the authors infer that cyclopentanol has the most compatible geometry and volume for the remaining space within the cyclodextrin cavity after inclusion of pyrene. With the larger *γ*-cyclodextrin, two pyrene molecules can be accommodated within the cavity. When a pyrene moiety is covalently linked to *γ*-cyclodextrin

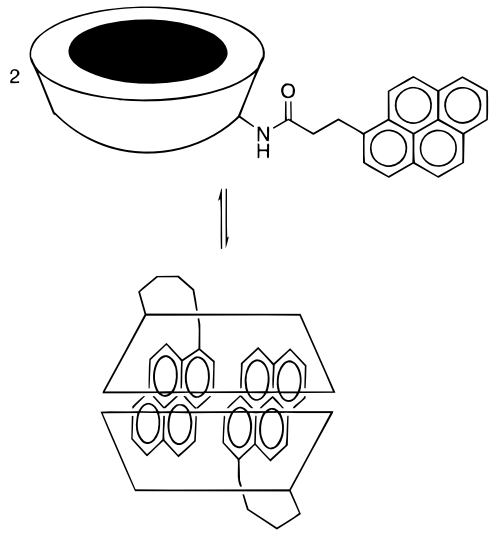


**Figure 48.** Pyrene-linked $\gamma$-cyclodextrin dimerizes in aqueous solution.

at the narrow rim, through an amine derived from one of the primary hydroxyls, a 2:2 inclusion complex forms (Figure 48).[105] Examination of the absorption spectrum of pyrene-linked $\gamma$-cyclodextrin led to the determination of a dissociation constant of 5.7 $\mu$M in 10% DMSO/water. When a bulky molecule (*e.g.*, cyclododecanol, menthol, borneol) is added to this complex, the aggregate dissociates so that the guest may be included in the cyclodextrin cavity. The resultant changes in the fluorescence spectrum of pyrene led the authors to suggest the use of this system as a sensor molecule. Similar behavior was also observed for nonlinked pyrenylbutyrate and $\gamma$-cyclodextrin by Farid and co-workers.[106] One of the two pyrene molecules in the 2:2 pyrene:cyclodextrin aggregate could be replaced by an amphiphilic molecule such as sodium hexanesulfonate, preventing quenching of excited pyrene.[107]

Nolte and co-workers have recently described an intriguing receptor system that exploits hydrophobic interactions to drive complexation between cyclodextrin molecules and porphyrins.[108] A ditopic receptor featuring two $\beta$-cyclodextrin moieties linked by bipyridyl units (Figure 49) was found to form a 2:2 complex with tetraaryl porphine **7** (Figure 14). The driving force for this assembly is the insertion of the benzoic acid moieties of the porphyrin into the cyclodextrin cavities. Fluorescence intensity titrations were used to determine a dissociation constant of no more than 20 nM in neutral aqueous solution. This titration was performed in the presence of zinc ions, which were found to facilitate the assembly process and to increase the rigidity of the resultant aggregate. Evidence for these two effects came from $^1$H NMR studies which showed line sharpening upon addition of zinc ions and titration studies which showed increased cooperativity in assembly. The zinc effect was coupled with evidence from gel filtration, $^1$H NMR spectroscopy, and molecular modeling to support assignment of the 2:2 stoichiometry (Figure 50).

## *IV. Metal-Templated Systems*

Metal−ligand interactions are both strong and architecturally diverse, enabling the construction of

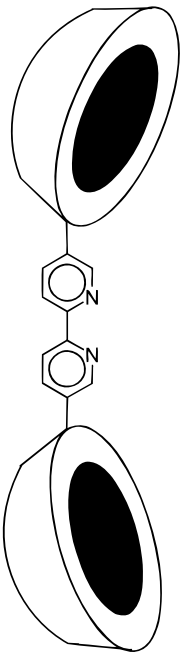


**Figure 49.** Bipyridyl-linked bis(cyclodextrin) receptor.

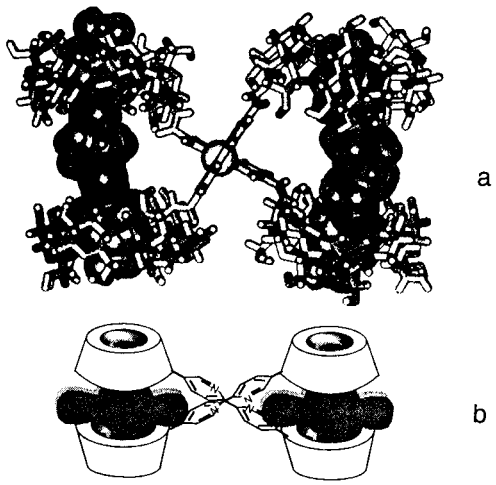


**Figure 50.** A 2:2 complex of tetraaryl porphyrin and ditopic cyclodextrin. (Reprinted with permission from reference 108. Copyright American Chemical Society.)

multisubunit assemblies. Aggregates that are organized by metal−ligand interactions are generally more amenable to X-ray crystal structure determination than their all-organic counterparts, probably by virtue of the greater ionic character of the complexes. The strength of metal−ligand noncovalent interactions allows many of these systems to aggregate in aqueous solution. Consequently, the study of self-assembly through the exploitation of metal−ligand interactions is well developed,[1,2,5,109] although the similarity of these systems to biological self-assembling aggregates is much more tangential. The discussion here will focus on the assembly of discrete, soluble aggregates that encapsulate guest molecules.

### A. Two Ligand Systems

One of the earliest examples of a metal-organized self-assembling receptors were reported by Maverick and co-workers.[110−113] In these complexes, two ditopic acac-derived ligands form a macrocycle with two metal ions. Cu(II), Ni(II), and Pd(II) were used,[112] although most complexation studies were performed

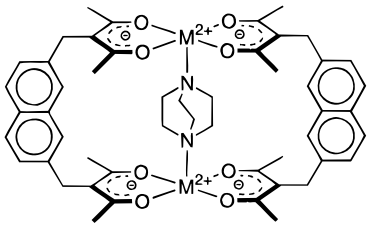

**Figure 51.** Ditopic binding within a copper-chelated macrocycle.

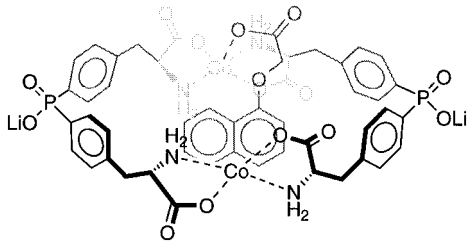

**Figure 52.** Self-assembly of a cyclophane receptor by metal complexation.

using Cu(II) because of the ease of monitoring titrations by visible spectroscopy. In particular, the receptor with a naphthalene spacer was found to have a usefully large cavity between the two metals (7.35 Å, Figure 51). The coordinated macrocycle readily forms in aqueous solution and was studied by $^1$H NMR and X-ray crystallography. Nitrogenous bases interact strongly with the Cu(II) centers in chloroform solution, giving a characteristic spectrophotometric change. Diaza ligands (*i.e.* pyrazine, dabco) display enhanced affinity as a result of inclusion within the macrocycle by simultaneous interaction with both copper ions. X-ray crystal structures of the macrocycle with dabco[111] and 2,5-dimethylpyrazine[113] conclusively demonstrate this internal coordination. The two copper ions are brought somewhat closer together (7.4 Å) as a result of simultaneous chelation with dabco while this distance increases when 2,5-dimethylpyrazine is bound within the cavity. The strain produced by this, as well as the reduced basicity of the nitrogen atoms, was given as explanation for the reduced affinity of pyrazine ($K_d$ = 0.2 M) relative to dabco ($K_d$ = 4.5 mM).[113] These results were reflected in thermodynamic parameters of binding. Dabco interacts with the macrocycle with favorable enthalpy (−7.2 kcal/mol) and unfavorable entropy (−12 cal/K·mol). In contrast, pyrazine shows a slightly less favorable enthalpy of binding (−6.7 kcal/mol) and even more unfavorable entropy of binding (−19 cal/K·mol). On the other hand, 2-aminopyrazine showed greater affinity for the cleft ($K_d$ = 11 mM).[113] The authors attributed this increased affinity to hydrogen-bonding interactions between the $NH_2$ of the amino group and the oxygen atoms coordinated to the metal ion, although no further spectroscopic changes were seen and crystallographic data was not given.

Schwabacher and co-workers have developed an elegant, self-assembling receptor for bicyclic aromatics in water (Figure 52).[114,115] Metal binding by the bis(amino acid) receptors forms a macrocycle with the ideal shape for indole and napthalene derivatives. Dissociation constants were measured by $^1$H NMR titration to be as low as 165 $\mu$M in pD 9 borate buffer. In addition to the predominant hydrophobic effect,

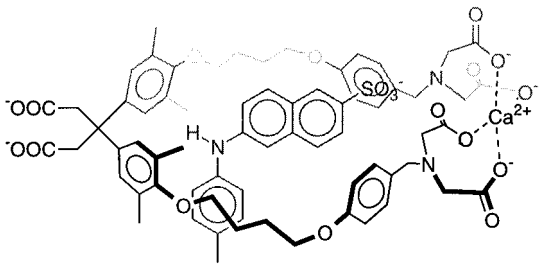

**Figure 53.** Self-organization of a cyclophane receptor by metal complexation.

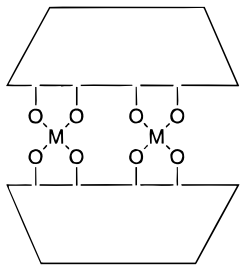

**Figure 54.** Metal complexation drives formation of a closed cyclodextrin shell.

substrates with a pendant carboxylate can participate in additional metal−ligand interactions. This ditopic mode of binding provides both stability and specificity to the complexation process.

Deshayes and co-workers have reported a similar type of self-organizing cyclophane receptor (Figure 53).[116] In this case, the receptor is covalently linked and calcium ion serves only to restrain the receptor to a productive conformation. This receptor is soluble in water and bound to 6-toluidino-2-naphthalenesulfonic acid (TNS) with a dissociation constant of 200 $\mu$M in 10 mM $CaCl_2$, pH 9.5. A shorter receptor, with only three carbons in the aliphatic chain, had a higher affinity for calcium, but was too small to fully enclose TNS. The ability of the receptor to bind TNS was removed in the presence of EDTA, which sequestered calcium ions. Despite the EDTA-like functionality of the receptor, affinity for calcium is somewhat modest and saturates only at 10 mM. At higher concentrations, there is an apparent change in structure causing release of TNS.

Much as macrocyclic structures can be brought together to form closed shells using hydrogen bonding (*vide supra*), complexation by metal ions can be used to bring together cyclodextrin rings.[117,118] When deprotonated by hydroxide in aqueous solution, cyclodextrins act as multidentate ligand to metal ions, forming closed-shell complexes (Figure 54). The complexes of $\beta$-cyclodextrin with copper[117] and $\gamma$-cyclodextrin with lead[118] have been revealed by X-ray crystallography to have extensive networks of metal−oxygen interactions. In the first complex, four cupric ions and 11 lithium ions zipper together the two cyclodextrin rings. Although there is some evidence that polyols form stable complexes with metal ions in aqueous solution, no evidence was given to support the existence of this complex outside of the solid state. The crystal structure of $\gamma$-cyclodextrin with lead showed the presence of 16 lead atoms at the interface between the two macrocycles. This indicates that all 16 secondary alcohols of each cyclodextrin have been deprotonated. This complex was not soluble in aqueous solution; at low temperatures, it

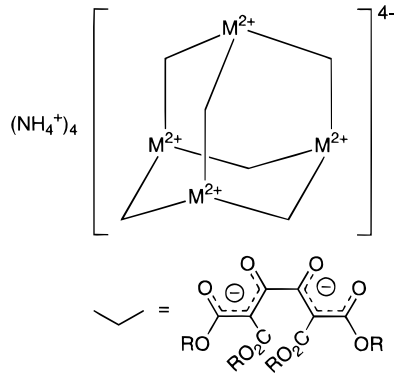

**Figure 55.** Tetrahedral complexes formed by metal−ligand interactions.

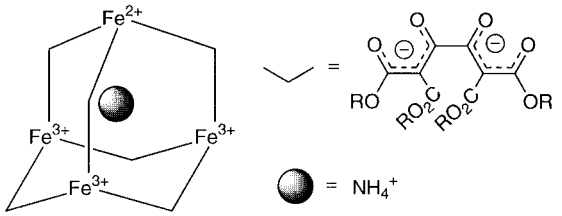

**Figure 56.** A neutral mixed-valence tetrahedral iron complex with encapsulated ammonium ion.

forms a voluminous gel and at high temperatures (75 °C), it crystallizes from solution. The complexation ability of these assemblies was, unfortunately, not discussed.

## B. Multicomponent Systems

Saalfranks' group has synthesized a number of tetrahedral multicomponent metal−ligand aggregates with central cavities (Figure 55).[119−123] They used a number of different metals in the self-assembly of these malonate complexes: Mg(II), Mn-(II), Co(II), Ni(II), Zn(II), and Fe(II/III). The assemblies were characterized by X-ray crystallography, elemental analysis, and FAB-MS. The symmetry of the aggregates is such that the $^1$H and $^{13}$C NMR spectra were uninformative. Nonetheless, solution-phase spectroscopy indicated that the assemblies spontaneously form in aqueous solution. In the case of the iron-based assembly derived from ligand A (Figure 55), the complex was obtained as a mixed valence complex with included ammonium ion (Figure 56).[122] Despite the increased cavity size resulting from the use of longer spacers, no mention was made of the ability of these shells to include larger guests.

Fujita and co-workers have reported a number of metal-directed self-assembling receptors based upon palladium−pyridine interactions.[124−128] A simple receptor was assembled from flexible bis(4-pyridyl) units and palladium(II) (Figure 57) and was characterized by X-ray crystallography.[125] The ethylenediamine capping groups are vital to the assembly of a discrete species; absence of this ligand would permit infinite polymeric arrays. The two-dimensional receptor preferentially binds electron-rich benzene derivatives in aqueous solution ($D_2O$). The dissociation constants for 1,3,5-trimethoxybenzene and *p*-dinitrobenzene were reported as 400 and 33 $\mu$M, respectively. Guests of intermediate electron-density predictably bound with intermediate affinity. However, the receptor showed poor affinity for guests of

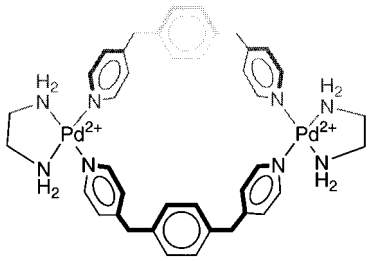

**Figure 57.** Pyridyl−palladium recognition is used to assemble a simple cyclophane receptor.

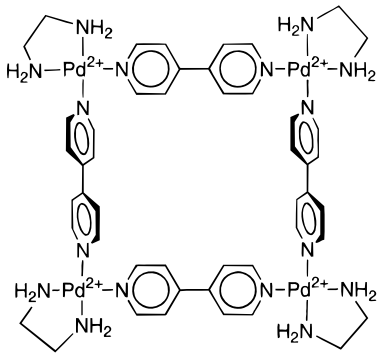

**Figure 58.** A molecular square.

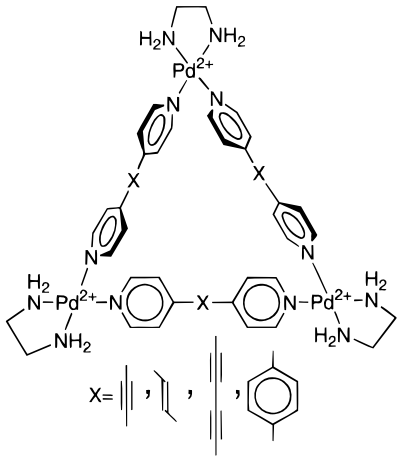

**Figure 59.** Increased flexibility in the bipyridyl ligand will allow formation of triangular structures.

any larger size ($K_d$ for *N*-(2-naphthyl)acetamide was 67 mM). An earlier related receptor, a molecular square based on four 4,4′-bipyridyl spacers, showed much greater affinity for napthalene derivatives with a dissociation constant of 556 $\mu$M (Figure 58).[124] Fujita and co-workers have recently published an analysis of the structural features of this molecular square,[128] giving X-ray crystallographic, ES-MS, elemental analysis, and $^1$H NMR data all supporting the assigned square geometry. This work also described important studies of the conformational consequences of longer bis(pyridyl) units: rather than existing as larger molecular squares, the shape of the "spacers" allows for a significant proportion of a triangular aggregate (Figure 59). This effect was also seen with a 4,4′-bipyridyl unit when the ethylenediamine capping ligand was replaced with bulkier 2,2′-bipyridyl group. Presumably steric clash between the two bipyridyl units is relieved in the triangular aggregate.

Stang and co-workers have also studied square assemblies of this type.[129−131] They used a combina-

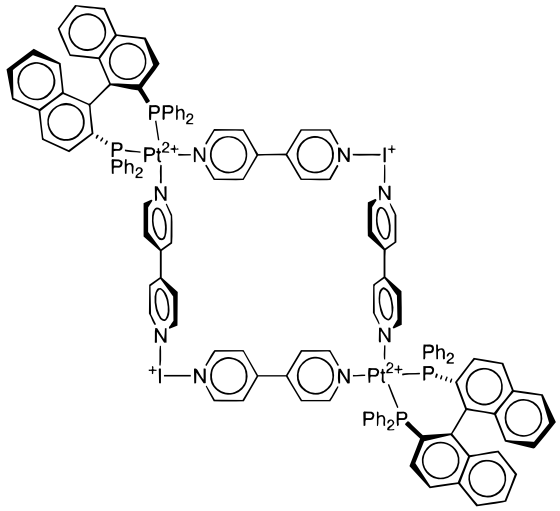

**Figure 60.** Mixed iodonium and platinum(II) complexation to produce molecular squares.

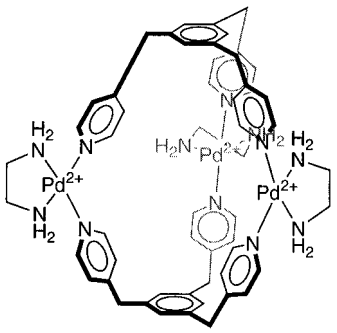

**Figure 61.** Cage formation is induced by guest binding.

tion of transition metals, Pd(II) and Pt(II), and iodonium ions coordination to prepare these assemblies (Figure 60). By using large, rigid linear spacers (*e.g.* diazaanthracene[129] or linear Pt(II)−phenyl−acetylene rods[130]), they have constructed molecular squares with diagonal dimension greater than 4 nm. Like many other groups who are interested in advancing analytical techniques in supramolecular chemistry, Stang and co-workers report the use of a gentle ionization technique (FAB-MS) for characterizing their large cationic aggregates.[131]

Fujita and co-workers have since turned their attention to larger, more complex systems. They have described an assembly consisting of three palladium atoms and two tris-pyridyl ligands (Figure 61) that forms in water only in the presence of an appropriate guest, a prime example of "induced-fit" molecular recognition.[126] Evidence for the formation of the complex was derived from $^1$H NMR studies, ES-MS, and elemental analysis. The guests giving the highest yield of the cage complex (>90%) had both bulky hydrophobic groups and a carboxylate group (*e.g.*, 1-adamantanecarboxylic acid and 2-phenylpropionic acid). There was some limit on the geometrical constraints of the guest—(1-naphthyl)-acetate was only moderately effective as a template. Neutral guests (*e.g.*, *p*-xylene) were also effective (72% yield) but cationic guests were not.

Another spectacular example of the potential for the construction of three-dimensional nanometer-scale structures comes from the group of Fujita.[127] An adamantane-shaped complex was generated from six palladium atoms and four rigid tris(pyridyl) ligands by spontaneous assembly in aqueous solution (Figure 62). Again, ethylenediamine ligands were used to cap the palladium atoms and prevent the formation of polymeric arrays; higher order aggregates were not observed. The supramolecule was observed in solution by $^1$H NMR and characterized in the solid state with four bound molecules of 1-adamantanecarboxylic acid. The authors did not observe any complexes containing less that four molecules of 1-adamantanecarboxylic acid and concluded that an allosteric effect was operating. That is, inclusion of each adamantyl group further enhances the hydrophobicity of the chamber so that only completely occupied and unoccupied complex was observed during titration. This supramolecule is large enough to act like a particle, as was demonstrated by laser light scattering from which a mean diameter of 1.5 nm was measured. This value corresponded well with the predicted 1.9 nm Pd−Pd distance. Even larger supramolecules, characterized by $^1$H NMR, were constructed by inserting phenyl or biphenyl spacers between the pyridyl and triazine moieties. These assemblies were predicted to have Pd−Pd distances of 3.3 and 4.6 nm, respectively.

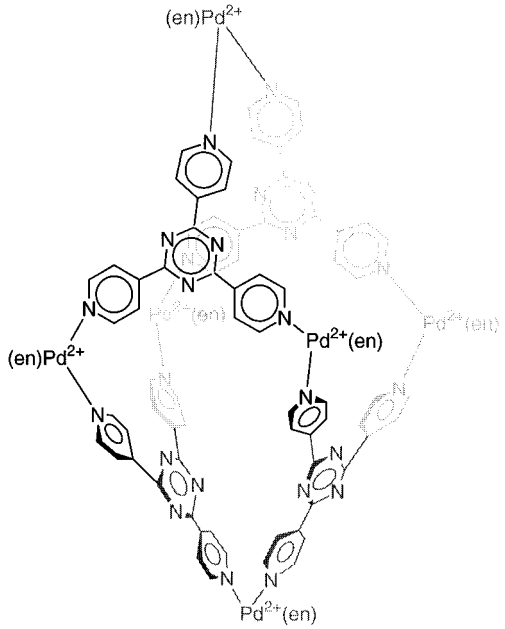

**Figure 62.** Nanometer-sized hosts (en = ethylenediamine).

## *V. Conclusion*

In conclusion, the behavior and functions of molecular assemblies can, to some extent, be controlled—either by solvation effects or nucleation by guests. The energetics for such complexes invariably pit intermolecular forces against the decreased freedom of the included guest. These forces are the van der Waals interactions and hydrogen bonds between the exterior surface of the guest and the interior surface of the host. In addition, special entropic effects can emerge when more than one solvent molecule is present in the capsules and is displaced by the guest molecule.

The greatest challenge facing this field is the characterization of aggregate structure. As we have seen, the assemblies discussed here defy the normal

analytical tools of small-molecule chemistry by nature of their sheer magnitude. While NMR spectroscopy and vapor pressure osmometry provide only indirect evidence for the formation of discrete aggregates, X-ray crystallography, can be insurmountably difficult with large, loosely defined structures. Moreover, aggregation processes may differ in solution and in the solid state and, moreover, aggregation processes may differ in solution and in the solid state. There is a great promise in the use of gentle ionization techniques in mass spectrometry but much work needs to be done to use this technique for determining more than just molecular mass. To be sure, molecular recognition is a field aided by, if not born from, molecular modeling. There is little question that the ability to interactively query structural mutation has led to the ever increasing sophistication and complexity of artificial receptors.

So, what can be done with self-assembling receptors? In this review, we have seen systems that are approaching the materials barrier, other systems that are capable of acting as sensors for interesting molecules, and others that can act as catalysts. Given external control of encapsulation processes, there may even be some potential to use self-assembling (and disassembling) receptors as drug transport agents. Another possibility is the use of these systems for autocatalysis: molecules that fit together can frequently act as templates for their own formation, one of the fundamental features of a self-replicating system. In essence, self-assembling systems can do anything that we would want to do with molecular recognition, but, like the modularity of biological systems, in a much more synthetically economical fashion. As we gain better control over aggregation, we can predictably make larger and more useful assemblies with given properties more simply and reliably.

## VI. Acknowledgments

J.R. thanks the National Institutes of Health and the Skaggs Institute for Chemical Biology for the financial support of research described in this review. M.M.C. is supported by a Camille and Henry Dreyfus Faculty Start-up Grant. We thank the reviewers of this manuscript for helpful suggestions.

## VII. References

(1) *Comprehensive Supramolecular Chemistry*; Lehn, J.-M., Atwood, J. L., Davies, J. E. D., MacNicol, D. D., Vögtle, F., Ed.; Pergamon: New York, 1996.
(2) Lawrence, D. S.; Jiang, T.; Levett, M. *Chem. Rev.* **1995**, *95*, 2229−2260.
(3) Philp, D.; Stoddart, J. F. *Angew. Chem., Int. Ed. Engl.* **1996**, *35*, 1154−1196.
(4) Jeffrey, G. A.; Saenger, W. *Hydrogen Bonding in Biological Structures*; Springer-Verlag: Berlin, 1991.
(5) Lehn, J. M. *Angew. Chem., Int. Ed. Engl.* **1990**, *29*, 1304−1319.
(6) Lindsey, J. S. *New J. Chem.* **1991**, *15*, 153−180.
(7) Whitesides, G. M.; Mathias, J. P.; Seto, C. T. *Science* **1991**, *254*, 1312−1319.
(8) Zimmerman, S. C.; Duerr, B. F. *J. Org. Chem.* **1992**, *57*, 2215−2217.
(9) Zimmerman, S. C.; Zeng, F.; Reichert, D. E. C.; Kolotuchin, S. V. *Science* **1996**, *271*, 1095−1098.
(10) Zimmerman, S. C.; Saionz, K. W.; Zeng, Z. *Proc. Natl. Acad. Sci. USA* **1993**, *90*, 1190−1193.
(11) Issberner, J.; Moors, R.; Vögtle, F. *Angew. Chem., Int. Ed. Engl.* **1995**, *33*, 2413−2420.
(12) Tomalia, D. N. *Sci. Am.* **1995**, *272*, 62−66.
(13) Hartgerink, J. D.; Granja, J. R.; Milligan, R. A.; Ghadiri, M. R. *J. Am. Chem. Soc.* **1996**, *118*, 43−50.
(14) Ghadiri, M. R.; Granja, J. R.; Buehler, L. K. *Nature* **1994**, *369*, 301−304.
(15) Granja, J. R.; Ghadiri, M. R. *J. Am. Chem. Soc.* **1994**, *116*, 10785−10786.
(16) Yoder, M. D.; Keen, N. T.; Jurnak, F. *Science* **1993**, *260*, 1503−1507.
(17) Raetz, C. R. H.; Roderick, S. L. *Science* **1995**, *270*, 997−1000.
(18) Ghadiri, M. R.; Kobayashi, K. G., J. R.; Chadha, R. K.; McRee, D. E. *Angew. Chem., Int. Ed. Engl.* **1995**, *34*, 93−95.
(19) Kobayashi, K.; Granja, J. R.; Ghadiri, M. R. *Angew. Chem., Int. Ed. Engl.* **1995**, *34*, 95−98.
(20) Clark, T. D.; Ghadiri, M. R. *J. Am. Chem. Soc.* **1995**, *117*, 12364−12365.
(21) Anderson, S.; Anderson, H. L.; Sanders, J. K. M. *Acc. Chem. Res.* **1993**, *26*, 469−475.
(22) Hoss, R.; Vögtle, F. *Angew. Chem., Int. Ed. Engl.* **1994**, *33*, 375−384.
(23) Zerkowski, J. A.; MacDonald, J. C.; Seto, C. T.; Wierda, D. A.; Whitesides, G. M. *J. Am. Chem. Soc.* **1994**, *116*, 2382−2391.
(24) Whitesides, G. M.; Simanek, E. E.; Mathias, J. P.; Seto, C. T.; Chin, D. N.; Mammen, M.; Gordon, D. M. *Acc. Chem. Res.* **1995**, *28*, 37−44.
(25) Seto, C. T.; Whitesides, G. M. *J. Am. Chem. Soc.* **1990**, *112*, 6409−6411.
(26) Seto, C. T.; Whitesides, G. M. *J. Am. Chem. Soc.* **1993**, *115*, 1330−1340.
(27) Mathias, J. P.; Simanek, E. E.; Zerowski, J. A.; Seto, C. T.; Whitesides, G. M. *J. Am. Chem. Soc.* **1994**, *116*, 4316−4325.
(28) Mathias, J. P.; Simanek, E. E.; Whitesides, G. M. *J. Am. Chem. Soc.* **1994**, *116*, 4326−4340.
(29) Seto, C. T.; Whitesides, G. M. *J. Am. Chem. Soc.* **1991**, *113*, 712−713.
(30) Seto, C. T.; Whitesides, G. M. *J. Am. Chem. Soc.* **1993**, *115*, 905−916.
(31) Seto, C. T.; Mathias, J. P.; Whitesides, G. M. *J. Am. Chem. Soc.* **1993**, *115*, 1321−1329.
(32) Mathias, J. P.; Seto, C. T.; Simanek, E. E.; Whitesides, G. M. *J. Am. Chem. Soc.* **1994**, *116*, 1725−1736.
(33) Mathias, J. P.; Simanek, E. E.; Seto, C. T.; Whitesides, G. M. *Angew. Chem., Int. Ed. Engl.* **1993**, *32*, 1766−1769.
(34) Mammen, M.; Simanek, E. E.; Whitesides, G. M. *J. Am. Chem. Soc.* **1996**, *118*, 12614−12623.
(35) Russell, K. C.; Leize, E.; Van Dorsselaer, A.; Lehn, J.-M. *Angew. Chem., Int. Ed. Engl.* **1995**, *34*, 209−213.
(36) Cheng, X.; Gao, Q.; Smith, R. D.; Simanek, E. E.; Mammen, M.; Whitesides, G. M. *J. Org. Chem.* **1996**, *61*, 2204−2206.
(37) Vreekamp, R. H.; van Duynhoven, J. P. M.; Hubert, M.; Verboom, W.; Reinhoudt, D. N. *Angew. Chem., Int. Ed. Engl.* **1996**, *35*, 1215−1218.
(38) Zhao, S.; Luong, J. H. T. *J. Chem. Soc., Chem. Commun.* **1994**, 2307−2308.
(39) Zhao, S.; Luong, J. H. T. *J. Chem. Soc., Chem. Commun.* **1995**, 663−664.
(40) Cram, D. J.; Jaeger, R.; Deshayes, K. *J. Am. Chem. Soc.* **1993**, *1993*, 10111−10116.
(41) Houk, K. N.; Nakamura, K.; Sheu, C.; Keating, A. E. *Science* **1996**, *273*, 627−629.
(42) Sheu, C.; Houk, K. N. *J. Am. Chem. Soc.* **1996**, *118*, 8056−8070.
(43) Cram, D. J.; Tanner, M. E.; Thomas, R. *Angew. Chem., Int. Ed. Engl.* **1991**, *30*, 1024−1027.
(44) Robbins, T. A.; Cram, D. J. *J. Am. Chem. Soc.* **1993**, *115*, 12199.
(45) Kurdistani, S. K.; Helgeson, R. C.; Cram, D. J. *J. Am. Chem. Soc.* **1995**, *117*, 1659−1660.
(46) Farrán, A.; Deshayes, K.; Matthews, C.; Balanescu, I. *J. Am. Chem. Soc.* **1995**, *117*, 9614−9615.
(47) Farrán, A.; Deshayes, K. D. *J. Phys. Chem.* **1996**, *100*, 3305.
(48) Parola, A. J.; Pina, F.; Ferreira, E.; Maestri, M.; Balzani, V. *J. Am. Chem. Soc.* **1996**, *118*, 11610−11616.
(49) Cram, D. J.; Cram, J. M. *Container Molecules and Their Guests*; Royal Society of Chemistry: Cambridge, 1994.
(50) Chapman, R. G.; Chopra, N.; Cochien, E. D.; Sherman, J. C. *J. Am. Chem. Soc.* **1994**, *116*, qq.
(51) Chapman, R. G.; Sherman, J. C. *J. Am. Chem. Soc.* **1995**, *117*, 9081−9082.
(52) Shinkai, S. *Tetrahedron* **1993**, *49*, 8933−8968.
(53) Linnane, P.; Shinkai, S. *Chem. Ind.* **1994**, *811*−814.
(54) Böhmer, V. *Angew. Chem., Int. Ed. Engl.* **1995**, *34*, 713−745.
(55) Gutsche, C. D. *Aldrichimica Acta* **1995**, *28*, 3−9.
(56) van Wageningen, A. M. A.; Verboom, W.; Reinhoudt, D. N. *Pure Appl. Chem.* **1996**, *68*, 1273−1277.
(57) Vreekamp, R. H.; Verboom, W.; Reinhoudt, D. N. *J. Org. Chem.* **1996**, *61*, 4282−4288.
(58) Koh, K.; Araki, K.; Shinkai, S. *Tetrahedron Lett.* **1994**, *35*, 8255−8258.
(59) Shimizu, K. D.; Rebek, J., Jr. *Proc. Natl. Acad. Sci. U.S.A.* **1995**, *92*, 12403−12407.
(60) Hamann, B. C.; Shimizu, K. D.; Rebek, J., Jr. *Angew. Chem., Int. Ed. Engl.* **1996**, *35*, 1326−1329.

(61) Etter, M.; Urbañczyk-Lipkowska, Z.; Zia-Ebrahimi, M.; Panunto, T. W. *J. Am. Chem. Soc.* **1990**, *112*, 8415−8426.
(62) Castellano, R. K.; Rudkevich, D. M.; Rebek, J., Jr. *J. Am. Chem. Soc.* **1996**, *118*, 10002−10003.
(63) Mogck, O.; Böhmer, V.; Vogt, W. *Tetrahedron* **1996**, *52*, 8489−8496.
(64) Böhmer, V. Personal communication, 1996.
(65) Scheerder, J.; Vreekamp, R. H.; Engbersen, J. F. J.; Verboom, W.; van Duynhoven, J. P. M.; Reinhoudt, D. N. *J. Org. Chem.* **1996**, *61*, 3476−3481.
(66) Kikuchi, Y.; Tanaka, Y.; Sutarto, S.; Kobayashi, K.; Toi, H.; Aoyama, Y. *J. Am. Chem. Soc.* **1992**, *114*, 10302−10306.
(67) Mock, W. L. *Top. Curr. Chem.* **1995**, *175*, 1.
(68) Jeon, Y.-M.; Kim, J.; Whang, D.; Kim, K. *J. Am. Chem. Soc.* **1996**, *118*, 9790−9791.
(69) Wyler, R.; de Mendoza, J.; Rebek, J. J. *Angew. Chem., Int. Ed. Engl.* **1993**, *32*, 1699−1701.
(70) Mohamadi, F.; Richards, N. G.; Guida, W. C.; Liskamp, R.; Lipton, M.; Caufield, C.; Chang, G.; Hendrickson, T.; Still, W. C. *J. Comput. Chem.* **1990**, *11*, 440−467.
(71) Valdés, C.; Spitz, U. P.; Toledo, L.; Kubik, S.; Rebek, J. J. *J. Am. Chem. Soc.* **1995**, *117*, 12733−12745.
(72) Branda, N.; Wyler, R.; Rebek, J. J. *Science* **1994**, *263*, 1267−1268.
(73) Garcias, X.; Rebek, J. J. *Angew. Chem., Int. Ed. Engl.* **1996**, *35*, 1225−1227.
(74) Fox, T.; Thomas, B. E., IV; McCarrick, M.; Kollman, P. A. *J. Phys. Chem.* **1996**, *100*, 10779−10783.
(75) Branda, N.; Grotzfeld, R. M.; Valdés, C.; Rebek, J., Jr. *J. Am. Chem. Soc.* **1995**, *117*, 85−88.
(76) Meissner, R.; de Mendoza, J.; Rebek, J. J. *Science* **1995**, *270*, 1485−1488.
(77) Meissner, R.; Garcias, X.; Mecozzi, S.; Rebek, J. J. *J. Am. Chem. Soc.* **1997**, *119*, 77−85.
(78) Kang, J.; Rebek, J., Jr. *Nature* **1996**, *382*, 239−241.
(79) Kang, J.; Rebek, J. J. *Nature* **1997**, *385*, 50−52.
(80) Grotzfeld, R.; Branda, N.; Rebek, J., Jr. *Science* **1996**, *271*, 487−489.
(81) Muehldorf, A. V.; Van Engen, D.; Warner, J. C.; Hamilton, A. D. *J. Am. Chem. Soc.* **1988**, *110*, 6561−6562.
(82) Gowsami, S.; Hamilton, A. D.; Van Engen, D. *J. Am. Chem. Soc.* **1989**, *111*, 3425−3426.
(83) Adrian, J. C., Jr.; Wilcox, C. S. *J. Am. Chem. Soc.* **1989**, *111*, 8055−8057.
(84) Askew, B.; Ballester, P.; Buhr, C.; Jeong, K. S.; Jones, S.; Parris, K.; Williams, K.; Rebek, J., Jr. *J. Am. Chem. Soc.* **1989**, *111*, 1082−1090.
(85) Williams, K.; Askew, B.; Ballester, P.; Buhr, C.; Jeong, K. S.; Jones, S.; Rebek, J., Jr. *J. Am. Chem. Soc.* **1989**, *111*, 1090−1094.
(86) Galán, A.; de Mendoza, J.; Toiron, C.; Bruix, M.; Deslongchamps, G.; Rebek, J., Jr. *J. Am. Chem. Soc.* **1991**, *113*, 9424−9425.
(87) Park, T. K.; J., S.; Rebek, J., Jr. *J. Am. Chem. Soc.* **1991**, *113*, 5125−5127.
(88) Park, T. K.; Schroeder, J.; Rebek, J., Jr. *Tetrahedron* **1991**, *47*, 2507−2518.
(89) Conn, M. M.; Deslongchamps, G.; de Mendoza, J.; Rebek, J., Jr. *J. Am. Chem. Soc.* **1993**, *115*, 3548−3557.
(90) Kato, Y.; Conn, M. M.; Rebek, J., Jr. *J. Am. Chem. Soc.* **1994**, *116*, 3279−3284.
(91) Furata, H.; Magda, D.; Sessler, J. L. *J. Am. Chem. Soc.* **1991**, *113*, 978−985.
(92) Zimmerman, S. C.; Wu, W.; Zeng, Z. *J. Am. Chem. Soc.* **1991**, *113*, 196−201.
(93) Schall, O. F.; Gokel, G. W. *J. Am. Chem. Soc.* **1994**, *116*, 6089−6100.
(94) Sessler, J. L.; Wang, R. *J. Am. Chem. Soc.* **1996**, *118*, 9808−9809.
(95) Harada, A.; Takahashi, S. *J. Chem. Soc., Chem. Commun.* **1988**, 1352−1353.
(96) Davies, D. M.; Deary, M. E. *J. Chem. Soc., Perkin Trans. 2* **1995**, 1287−1294 and references therein.
(97) Andersson, T.; Nilsson, K. S., M.; Westman, G.; Wennerstrom, O. *J. Chem. Soc., Chem. Commun.* **1992**, 604−606.
(98) Yoshida, Z.; Takekuma, H.; Takekuma, S.; Matsubara, Y. *Angew. Chem., Int. Ed. Engl.* **1994**, *33*, 1597−1599.
(99) Boulas, P.; Kuntner, W.; Jones, M. T.; Kardish, K. M. *J. Phys. Chem.* **1994**, *98*, 1282−1287.
(100) Raston, C. L. In *Comprehensive Supramolecular Chemistry*; Gokel, G. W., Ed.; Elsevier: Oxford, 1996; Vol. 1, pp 777−787.
(101) Kim, H.-S.; Jeon, S.-J. *Chem. Commun.* **1996**, 817−818.
(102) Bodor, N.; Huang, M.-J.; Watts, J. D. *J. Inclusion Phenom. Mol. Recognit. Chem.* **1996**, *25*, 97−102.
(103) Koehler, G.; Grabner, G.; Klein, C. T. H.; Marconi, G.; Mayer, B.; Monti, S.; Recthaler, K.; Rotkiewicz, K.; Veirnstein, H.; Wolschann, P. *J. Inclusion Phenom. Mol. Recognit. Chem.* **1996**, *25*, 103−108.
(104) Muñoz de la Peña, A.; Ndou, T. T.; Zung, J. B.; Greene, K. L.; Live, D. H.; Warner, I. M. *J. Am. Chem. Soc.* **1991**, *113*, 1572−1577.
(105) Ueno, A.; Suzuki, I.; Osa, T. *J. Am. Chem. Soc.* **1989**, *111*, 6391−6397.
(106) Herkstroeter, W. G.; Martic, P. A.; Farid, S. *J. Chem. Soc., Perkin Trans. 2* **1984**, 1453−1457.
(107) Herkstroeter, w. G.; Martic, P. A.; Evans, T. R.; Farid, S. *J. Am. Chem. Soc.* **1986**, *108*, 3275−3280.
(108) Venema, F.; Rowan, A. E.; Nolte, R. J. M. *J. Am. Chem. Soc.* **1996**, *118*, 257−258.
(109) Pope, M. T.; Müller, A. *Angew. Chem., Int. Ed. Engl.* **1991**, *30*, 34−48.
(110) Maverick, A. W.; Klavetter, F. E. *Inorg. Chem.* **1984**, *23*, 4129−4130.
(111) Maverick, A. W.; Buckingham, S. C.; Yao, Q.; Bradbury, J. R.; Stanley, G. G. *J. Am. Chem. Soc.* **1986**, *108*, 7430−7431.
(112) Bradbury, J. R.; Hampton, J. L.; Martone, D. P.; Maverick, A. W. *Inorg. Chem.* **1989**, *28*, 2392−2399.
(113) Maverick, A. W.; Ivie, M. L.; Waggenspack, J. H.; Fronczek, F. R. *Inorg. Chem.* **1990**, *29*, 2403−2409.
(114) Lee, J.; Schwabacher, A. W. *J. Am. Chem. Soc.* **1994**, *116*, 8382−8383.
(115) Schwabacher, A. W.; Lee, J.; Lei, H. *J. Am. Chem. Soc.* **1992**, *114*, 7597−7598.
(116) Cole, K. L.; Farran, M. A.; Deshayes, K. *Tetrahedron Lett.* **1992**, *33*, 599−602.
(117) Fuchs, R.; Habermann, N.; Klüfers, P. *Angew. Chem., Int. Ed. Engl.* **1993**, *32*, 852−854.
(118) Klüfers, P.; Schuhmacher, J. *Angew. Chem., Int. Ed. Engl.* **1994**, *33*, 1863−1865.
(119) Saalfrank, R. W.; Stark, A.; Peters, K.; von Schnering, H. G. *Angew. Chem., Int. Ed. Engl.* **1988**, *27*, 851−853.
(120) Saalfrank, R. W.; Stark, A.; Bremer, M.; Hummel, H.-U. *Angew. Chem., Int. Ed. Engl.* **1990**, *29*, 311−314.
(121) Saalfrank, R. W.; Hörner, B.; Stalke, D.; Salbeck, J. *Angew. Chem., Int. Ed. Engl.* **1993**, *32*, 1179−1182.
(122) Saalfrank, R. W.; Burak, R.; Breit, A.; Stalke, D.; Herbt-Irmer, R.; Daub, J.; Porsch, M.; Bill, E.; Müther, M.; Trautwein, A. X. *Angew. Chem., Int. Ed. Engl.* **1994**, *33*, 1621−1623.
(123) Saalfrank, R. W.; Burak, R.; Reihs, S.; Löw, N.; Hampel, F.; Stachel, H.-D.; Lentmaier, J.; Peters, K.; Peters, E.-M.; von Schnering, H. G. *Angew. Chem., Int. Ed. Engl.* **1995**, *34*, 993−995.
(124) Fujita, M.; Yazaki, J.; Ogura, K. *Tetrahedron Lett.* **1991**, *32*, 5589.
(125) Fujita, M.; Nagao, S.; Iida, M.; Ogata, K.; Ogura, K. *J. Am. Chem. Soc.* **1993**, *115*, 1574−1576.
(126) Fujita, M.; Nagao, S.; Ogura, K. *J. Am. Chem. Soc.* **1995**, *117*, 1649−1650.
(127) Fujita, M.; Oguro, D.; Miyazawa, M.; Oka, H.; Yamaguchi, K.; Ogura, K. *Nature* **1995**, *378*, 469−471.
(128) Fujita, M.; Sasaki, O.; Mitsuhashi, T.; Fujita, T.; Yazaki, J.; Yamaguchi, K.; Ogura, K. *J. Chem. Soc., Chem. Commun.* **1996**, 1535−1536.
(129) Olenyuk, B.; Whiteford, J. A.; Stang, P. J. *J. Am. Chem. Soc.* **1996**, *118*, 8221−8230.
(130) Manna, J.; Whiteford, J. A.; Stang, P. J.; Muddiman, D. C.; Smith, R. D. *J. Am. Chem. Soc.* **1996**, *118*, 8731−8732.
(131) Whiteford, J. A.; Rachlin, E. M.; Stang, P. J. *Angew. Chem., Int. Ed. Engl.* **1996**, *35*, 2524−2529.

CR9603800